

RADIATIVE PROCESSES IN AN  
INTENSE MAGNETIC FIELD

Thesis by  
Donald Lionel Patrick Strange

In Partial Fulfillment of the Requirements  
for the Degree of  
Doctor of Philosophy

California Institute of Technology  
Pasadena, California

1972  
(Submitted May 15, 1972)

ACKNOWLEDGMENTS

The author would like to thank :-

Prof. P. Goldreich, for supervising this research;

the Woodrow Wilson Fellowship program, NATO, and Caltech, for their financial support;

Mr. and Mrs. D. Nickerson, for providing a home away from home;

Chris Luras, for dispensing much humour and medicine;

Keck House, for much fun and many friends.

# ABSTRACT

Three astrophysical problems relating to the intense magnetic fields associated with neutron stars (i.e.  $10^{12}$  gauss) and white dwarfs (i.e.  $10^8$  gauss) are studied.

(1) The radiation rate for non-relativistic bremsstrahlung in  $10^{12}$  gauss is computed by both quantum-mechanical and classical methods. The main features of this emissivity are a  $1/\rho_z$  dependence (magnetic field in the z-direction) characteristic of a one-dimensional momentum space, a larger flux perpendicular to  $\vec{B}$  than parallel to it, and a net left-handed polarization in the flux parallel to  $\vec{B}$ .

(2) The electron energy levels and orbits for hydrogen in  $10^{12}$  gauss are calculated with variational techniques. The ground state binding energy is found to be 200 ev. The other levels divide into a set of tightly bound states (binding energies 100 to 200 ev) and a double-set of hydrogen-like levels (0 to 13 ev). The overall electron density of the atom is elongated along the magnetic field direction. The thermal ionization fraction of a neutral hydrogen plasma is computed using an appropriately modified Saha equation, and is found to be 90%. Finally, high Z atoms are investigated via the Thomas-Fermi approximation with the result that the definitive equation is

$$\chi'' = \chi'^{1/2} z^{1/2}$$

giving an atomic radius of

$$R = 4 \times 10^{-5} Z^{1/5} a_0^{2/5} \text{ cm.}$$

(3) Cyclotron emission and absorption in a magnetic field of  $10^8$  gauss is studied as a possible mechanism for the observed degree of circular polarization in the optical emission from white dwarfs. A few simple models explain some of the quantitative and qualitative aspects of the polarization data.



TABLE OF CONTENTS

Acknowledgments	ii
Abstract	iii

Part I : NON-RELATIVISTIC ELECTRON BREMSSTRAHLUNG IN AN INTENSE  
MAGNETIC FIELD

Chapter 1 : INTRODUCTION	2
Chapter 2 : QUANTUM-MECHANICAL CALCULATION	5
2.1 An Electron in $10^{12}$ Gauss	5
2.2 Basic Formulation	8
2.3 The Coulomb Integrals	13
2.4 The Coefficients $C_{\mu}$	17
2.5 The Energy Denominators	19
2.6 The Matrix Element	20
2.7 Radiation Rates	22
2.8 Summations Over the Radial Quantum Number 's'	25
2.9 Some Polarization Aspects	29
Chapter 3 : CLASSICAL CALCULATION	30
Chapter 4 : CONCLUSIONS AND DISCUSSION	34
Appendix 1 : AMPLIFICATION CONDITION	35
Appendix 2 : THE RADIATION TERM	37
References	40

Part II : ATOMS IN AN INTENSE MAGNETIC FIELD

Chapter 5 : INTRODUCTION	42
Chapter 6 : HYDROGEN	46
6.1 A "Bohr" Picture	46
6.2 Truncated Coulomb Potential	50
6.3 Variational Calculation #1	54
6.4 Variational Calculation #2	59
Chapter 7 : IONIZATION FRACTION	65
7.1 Statistics	65
7.2 Ionization Fraction	70
Chapter 8 : A "THOMAS-FERMI" MODEL	75
Chapter 9 : CONCLUSIONS AND DISCUSSION	80
Figure 1	83
Figure 2	84
Figure 3	85
Table 1	86
Table 2	87
References	88

Part III : CYCLOTRON RADIATION IN AN INTENSE MAGNETIC FIELD

Chapter 10 : INTRODUCTION	90
Chapter 11 : THIN SHELL CYCLOTRON RADIATION	93
11.1 General Formulation	93

11.2 Hemispherical Shell and a Radial Magnetic Field	100
11.3 Hemispherical Shell and a Dipole-like Magnetic Field	101
11.4 A "Thin" Sheet	103
11.5 An "Atmosphere"	107
Chapter 12 : CONCLUSIONS AND DISCUSSION	114
Figure 1	116
Figure 2	117
Figure 3	118
Figure 4	119
Figure 5	120
Figure 6	121
Figure 7	122
References	123

-1-

Part I

NON-RELATIVISTIC ELECTRON BREMSSTRAHLUNG  
IN AN INTENSE MAGNETIC FIELD

## Chapter 1

### INTRODUCTION

Since the discovery (Hewish et al. 1968) of pulsars in 1967 and the subsequent hypothesis that they are rotating neutron stars (Gold 1968), considerable attention has been paid to the nature of physical processes in such an environment, primarily in the hope of explaining the pulsar phenomenon. With neutron star models suggesting densities as high as  $10^{15}$  gm/cm<sup>3</sup> (Cameron 1970), and magnetic fields as high as  $10^{12}$  gauss (Gunn and Ostriker 1969), we expect some marked differences from the usual earth or stellar regimes.

In a magnetic field electrons are characterized by a principal quantum number 'n', which relates directly to the electron's radius of gyration about a magnetic field line. A "magnetic transition" (Camuto et al. 1969) occurs when such an electron changes its 'n' either by itself (i.e. spontaneous radiation  $n \rightarrow n' + \gamma$ ,  $n' < n$  which is the discrete analog of synchrotron radiation), or by colliding with a nucleus (i.e. coulomb de-excitation).

$$n + (Z, A) \rightarrow n' + (Z, A) + \gamma$$

If however, the electron's principal quantum number is the same before and after a coulomb interaction with a nucleus, it is a continuum

process sometimes referred to as "electron bremsstrahlung" (Canuto et al. 1969).

At high magnetic fields on the order of  $10^{12}$  gauss, this bremsstrahlung process is characterized by the almost one-dimensional motion of the electrons. For non-relativistic energies the gyroradius is less than  $1 \text{ \AA}$ . This streaming property suggested this process as a possible mechanism for producing the observed pulsar radio emission. Chiu and Canuto (1969) calculated the emissivity using the free-particle Green's function and got

$$I(p, \omega, \theta) \approx \omega^{-2} p^5 \sin^2 \theta \quad (1.1)$$

The spectral index of -2 matched the available data but the  $\sin^2 \theta$  term was a problem as it meant no emissivity along the magnetic field as observed. Furthermore, bremsstrahlung alone couldn't account for the high intensity observed (brightness temperature  $\sim 10^{24} \text{ }^\circ\text{K}$ ). Coherent amplification was also needed.

This meant that the absorption coefficient must be negative for the bremsstrahlung process. Simon and Strange (1969) derived a necessary condition for such a negative absorption coefficient (see Appendix 1), namely

$$\frac{dI}{dp} < 0 \quad (1.2)$$

Clearly the  $I \sim p^5$  result does not satisfy this condition and bremsstrahlung appears ruled out as a suitable amplifiable process.

Chiu and Canuto (1970) however, made two corrections. An error was pointed out in the derivation of (1.2) and it was revised to

$$\frac{d}{dp} \left( \frac{I}{p} \right) < 0 \quad (1.3)$$

Furthermore they realized that the use of the free-particle Green's function limited their emissivity to high quantum numbers only, not the low 'n' one-dimensional region of interest.

I have therefore calculated the emissivity of a  $n=0$  (ground state) electron interacting with a nucleus via the bremsstrahlung process. The result is derived by two methods, one quantum-mechanical, the other classical.

## Chapter 2

### QUANTUM-MECHANICAL CALCULATION

#### 2.1 An Electron in $10^{12}$ Gauss

Non-relativistic electrons (kinetic energies on the order of 1 kev.) in a homogeneous magnetic field of about  $10^{12}$  gauss are considered. The electron state is characterized (Sokolov and Ternov 1968) by a principal quantum number 'n' (n 0,1,2,3,4....), a radial quantum number 's' (s 0,1,2,3,4....), and a momentum variable ' $p_z$ ' along the direction of the magnetic field  $\vec{H}$  (taken to be in the positive z-direction).

The electron's wave function is the solution to the Dirac equation and in cylindrical coordinates (r,  $\phi$ , z) is given by

$$\Psi_{nsp_z} = \frac{e^{\frac{i p_z z}{\hbar}}}{L} \frac{e^{i(l - \frac{1}{2})\phi}}{\sqrt{2\pi}} \sqrt{2\gamma} \begin{pmatrix} C_1 e^{-\frac{i\phi}{2}} I_{n-1,s}(\rho) \\ i C_2 e^{\frac{i\phi}{2}} I_{n,s}(\rho) \\ C_3 e^{-\frac{i\phi}{2}} I_{n-1,s}(\rho) \\ i C_4 e^{\frac{i\phi}{2}} I_{n,s}(\rho) \end{pmatrix} \quad (2.1)$$

where

$$l = n - s$$

$$\rho = \gamma r^2 \quad (2.2)$$



and 
$$\gamma = \frac{e \hbar}{2 c \hbar}$$

$I_{n,s}(\rho)$  is a generalized Laguerre function, and the coefficients  $C_\mu$  describe the spin and polarization state of the electron.

The total energy 'E' of the electron is

$$E(n, p_z) = \left[ m_e^2 c^4 + p_z^2 c^2 + 4 \gamma n \hbar^2 c^2 \right]^{1/2} \quad (2.3)$$

(neglecting the anomalous magnetic moment of the electron). For  $H \sim 10^{12}$  gauss, the  $n=1$  level is about 10 kev above the ground state  $n=0$  level.

The primary feature of such a ground state electron is its one-dimensional behaviour. The electron is essentially constrained to travel in a straight line parallel to the magnetic field. This is evident from the form of the  $n=0$  Laguerre function.

$$I_{0,s}(\rho) = \frac{(-1)^s e^{-\rho/2} \rho^{s/2}}{\sqrt{s!}} \quad (2.4)$$

Then

$$\left| \Psi_{0sp_z} \right|^2 \sim \frac{e^{-\rho} \rho^s}{s!} \quad (2.5)$$

This space probability function peaks at  $\rho=s$ , i.e.  $r = \sqrt{s/\gamma}$ . Thus the degenerate quantum number 's' designates the center of the particle's trajectory. For a magnetic field of  $10^{12}$  gauss, the "spacing" between

the possible trajectories is very small ( $\sqrt{r_g} \sim 3 \times 10^{-10}$  cm.). For small 's' the half-width of  $|\Psi|^2$  is of similar magnitude.

For  $n=0$  the electron can be thought of as spiralling about the trajectory center. The "radius" of the orbit is simply  $R = \sqrt{r_g}$ . Thus for low 'n' we still have a very constrained motion as the electron is confined to a tube, parallel to the magnetic field and having a diameter less than  $1 \text{ \AA}$ .

Because of this constraint we expect accelerations perpendicular to the magnetic field to be severely dampened. For such an electron interacting with a nucleus, the primary radiation producing acceleration is the push-pull along the trajectory, rather than the perpendicular deflection as in the case of ordinary bremsstrahlung.

## 2.2 Basic Formulation

An  $n=0$  electron interacting with the coulomb field of a stationary nucleus is considered. Bremsstrahlung is a second order process, thereby necessitating an intermediate state,  $n=0$  for the initial and final states, but this need not be the case for the intermediate one. There can be a virtual transition to and from a higher principal quantum number. This is a manifestation of the acceleration perpendicular to the magnetic field that takes place despite the one-dimensional nature of the electron's motion.

The transition probability rate is given (Heitler 1954) by Fermi's Golden Rule

$$W_{0 \rightarrow F} = \frac{2\pi}{\hbar} |K_{F0}|^2 \rho_F \quad (2.6)$$

where in the case of bremsstrahlung

$$K_{F0} = \sum_{I, II} \left( \frac{V_{FI} H_{I0}}{E_0 - E_I - \hbar\omega} + \frac{H_{FI} V_{II0}}{E_0 - E_{II}} \right) \quad (2.7)$$

$$H_{ba} = -e \sqrt{\frac{2\pi\hbar c}{\kappa}} \int \psi_b^* \alpha_e e^{-i\vec{\kappa} \cdot \vec{r}} \psi_a d^3x \quad (2.8)$$

$$V_{ba} = \int \psi_b^* \frac{Ze^2}{|\vec{r}|} \psi_a d^3x \quad (2.9)$$

The radiation term  $H_{ba}$  (derived in detail in Appendix 2) is given by

$$H_{nsp_z \rightarrow n's'p'_z} = -e \sqrt{\frac{2\pi\hbar c}{\kappa}} \vec{\alpha} \cdot \vec{e} \quad (2.10)$$

where  $\vec{e}$  is the photon polarization vector, and  $\vec{\alpha}$  is

$$\begin{aligned} \begin{pmatrix} \alpha_x \\ \alpha_y \end{pmatrix} &= \delta(p'_z + \hbar\kappa \cos \Theta - p_z) I_{ss'} \left[ \begin{pmatrix} i \\ 1 \end{pmatrix} (c'_4 c_4 + c'_2 c_2) I_{n,n'-1} + \begin{pmatrix} -i \\ 1 \end{pmatrix} (c'_4 c_1 + c'_2 c_3) I_{n-1,n'} \right] \\ \alpha_z &= \delta(p'_z + \hbar\kappa \cos \Theta - p_z) I_{ss'} \left[ (c'_3 c_1 + c'_1 c_3) I_{n-1,n'-1} - (c'_4 c_2 + c'_2 c_4) I_{n,n'} \right] \end{aligned} \quad (2.11)$$

The argument of the Laguerre functions is

$$\chi = \frac{\kappa^2 \sin^2 \Theta}{4\gamma} \quad (2.12)$$

where  $\vec{\kappa}$  is the photon propagation vector (taken to be in the YZ plane), and  $\Theta$  is the angle  $\vec{\kappa}$  makes with the magnetic field  $\vec{H}$ .

The coulomb term  $V_{ba}$  is

$$V_{nsp_z \rightarrow n's'p_z'} = \frac{2Ze^2}{L} \delta(l-l') \times$$

$$\int_0^\infty \left[ (C_1 C_1' + C_3 C_3') I_{n-1,s}(e) I_{n'-1,s'}(e) + (C_2 C_2' + C_4 C_4') I_{n,s}(e) I_{n',s'}(e) \right] K_0(\alpha e^{1/2}) de$$

(2.13)

where

$$\alpha = \frac{|p_z - p_z'|}{\hbar \gamma^{1/2}} \quad (2.14)$$

For pulsar radio emission ( $\omega \sim 10^8 \text{ sec}^{-1}$ ) in a field of  $\sim 10^{12}$  gauss, the argument  $\chi$  is very small. For small  $\chi$  (Sokolov and Ternov 1968)

$$I_{nn'}(\chi) \approx \sqrt{\frac{n!}{n'!}} \frac{1}{(n-n')!} \chi^{1/2(n-n')} \quad (2.15)$$

Therefore in the formulae for  $\bar{\alpha}_x$ ,  $\bar{\alpha}_y$ , and  $\bar{\alpha}_z$ , to first order we need only consider transitions that give rise to  $I_{00}$  terms. For  $\bar{\alpha}_x$  and  $\bar{\alpha}_y$  this means a  $0 \rightarrow 1$  or a  $1 \rightarrow 0$  transition. For  $\bar{\alpha}_z$  there is only the  $0 \rightarrow 0$  transition.

The six resulting transition terms are

$$\begin{aligned}
 H_{0 \rightarrow 1} &\approx -e \frac{2\pi\hbar c}{\kappa} \delta(p_z' + \hbar\kappa \cos\theta - p_z) \delta(s-s') (C_1' C_4 + C_3' C_2) (ie_x + e_y) \\
 H_{0 \rightarrow 0} &\approx -e \frac{2\pi\hbar c}{\kappa} \delta(p_z' + \hbar\kappa \cos\theta - p_z) \delta(s-s') (C_4' C_2 + C_2' C_4) e_z \\
 H_{1 \rightarrow 0} &\approx -e \frac{2\pi\hbar c}{\kappa} \delta(p_z' + \hbar\kappa \cos\theta - p_z) \delta(s-s') (C_4' C_1 + C_2' C_3) (-ie_x + e_y)
 \end{aligned}
 \tag{2.16}$$


$$\begin{aligned}
 V_{0 \rightarrow 1} &= \frac{2Ze^2}{L} \delta(-s-1+s') \int_0^\infty (C_2 C_2' + C_4 C_4') I_{0,s}(e) I_{1,s'}(e) K_0(\alpha e^{1/2}) de \\
 V_{0 \rightarrow 0} &= \frac{2Ze^2}{L} \delta(s-s') \int_0^\infty (C_2 C_2' + C_4 C_4') I_{0,s}(e) I_{0,s'}(e) K_0(\alpha e^{1/2}) de \\
 V_{1 \rightarrow 0} &= \frac{2Ze^2}{L} \delta(1-s-s') \int_0^\infty (C_2 C_2' + C_4 C_4') I_{1,s}(e) I_{0,s'}(e) K_0(\alpha e^{1/2}) de
 \end{aligned}
 \tag{2.17}$$

The above six terms indicate that four sequences are contributing.

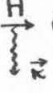
Using a (n,s) schemata, they are

$$\begin{aligned}
 (0,s) &\xrightarrow[\downarrow \kappa]{H} (0,s) \xrightarrow{V} (0,s) \\
 (0,s) &\xrightarrow{V} (0,s) \xrightarrow[\downarrow \kappa]{H} (0,s)
 \end{aligned}$$

$$(0, s) \xrightarrow[H]{\text{H}} (1, s) \xrightarrow{V} (0, s-1) \quad s \neq 0$$



$$(0, s) \xrightarrow{V} (1, s+1) \xrightarrow[H]{\text{H}} (0, s+1)$$



(2.18)

### 2.3 The Coulomb Integrals

The equations (2.17) contain three integrals where the integrand is a product of two Laguerre functions and a Bessel function. Using equation (2.4) and the fact that

$$L_{1,s}(e) = (-1)^s \frac{e^{-e/2} e^{\frac{s-1}{2}} (e-s)}{s!} \quad (2.19)$$

the required integrals are

$$J_{0 \rightarrow 1} = - \int_0^\infty \frac{e^{-e} e^s (e-s-1)}{s! (s+1)!} K_0(\alpha e^{1/2}) de \quad (2.20)$$

$$J_{0 \rightarrow 0} = \int_0^\infty \frac{e^{-e} e^s}{s!} K_0(\alpha e^{1/2}) de \quad (2.21)$$

$$J_{1 \rightarrow 0} = - \int_0^\infty \frac{e^{-e} e^{s-1} (e-s)}{s! (s-1)!} K_0(\alpha e^{1/2}) de \quad (2.22)$$

These forms can be evaluated using the integral relation  
(Gradshteyn and Ryzhik 1965)



$$\int_0^{\infty} x^{\nu} e^{-\delta x^2} K_{\nu}(\beta x) dx = \frac{1}{2} \delta^{-\frac{\nu}{2}} \beta^{-1} \Gamma\left(\frac{1+\nu}{2}\right) \Gamma\left(\frac{1-\nu}{2}\right)$$

$$x e^{\frac{\beta^2}{8\delta}} W_{-\frac{1}{2}\nu, \frac{1}{2}\nu}\left(\frac{\beta^2}{4\delta}\right)$$

(2.25)

$$\operatorname{Re} \mu > |\operatorname{Re} \nu| - 1$$

Putting

$$x^2 = e$$

$$\delta = 1$$

$$\nu = 0$$

$$\beta = \alpha$$

(2.26)

gives

$$\int_0^{\infty} e^{-e} e^{\frac{\nu-1}{2}} K_0(\alpha e^{\frac{\nu}{2}}) de = \alpha^{-1} \Gamma\left(\frac{1+\mu}{2}\right) \Gamma\left(\frac{1-\mu}{2}\right) e^{\frac{\alpha^2}{8}} W_{-\frac{1}{2}\mu, 0}\left(\frac{\alpha^2}{4}\right)$$

(2.27)

The Whittaker function  $W_{-\frac{1}{2}\mu, 0}$  can be written as an infinite series.

$$W_{-\frac{1}{2}\mu, 0}\left(\frac{\alpha^2}{4}\right) = \frac{\alpha e^{-\frac{\alpha^2}{8}}}{2 \left[\Gamma\left(\frac{\mu+1}{2}\right)\right]^2} \left\{ \sum_{k=0}^{\infty} \frac{\Gamma(k + \frac{\mu+1}{2})}{k! k!} \left(\frac{\alpha^2}{4}\right)^k \left[ 2\psi(k+1) - \psi\left(k + \frac{\mu+1}{2}\right) - \ln\left(\frac{\alpha^2}{4}\right) \right] \right\}$$

(2.28)

where 
$$\Psi(n+1) = -C + \sum_{k=1}^n \frac{1}{k} \quad (2.29)$$

'n' being a natural number and 'C' being Euler's number .5772157 .

The argument  $\frac{\alpha^2}{4}$  is very small for the regime being considered here. Conservation of energy gives

$$P_{2m}^2 - P_{2m}'^2 = \hbar\omega \quad (2.30)$$

i.e. 
$$\Delta P = \frac{\hbar\omega}{v} \quad (2.31)$$

for forward scattering. This combined with equation (2.14) gives

$$\alpha = \frac{\omega}{v\gamma^{1/2}} \approx 10^{-10} \quad (2.32)$$

for  $E \sim 1$  kev,  $\omega \sim 10^8$  sec<sup>-1</sup>, and  $\hbar \sim 10^{12}$  gauss.

Therefore, using only the k=0 term in the series expansion (2.28), equation (2.27) becomes

$$\int_0^\infty e^{-\epsilon} e^{\frac{\mu-1}{2}} K_0(\alpha e^{\frac{\mu}{2}}) d\epsilon \approx \frac{1}{2} \Gamma\left(\frac{\mu+1}{2}\right) \left[ 2\Psi(1) - \Psi\left(\frac{\mu+1}{2}\right) - \ln\left(\frac{\alpha^2}{4}\right) \right] \quad (2.33)$$

The integrals (2.20), (2.21), and (2.24) now reduce to

$$f_{0 \rightarrow 1} \approx -\frac{1}{2} \frac{1}{\sqrt{s+1}} \quad (2.34)$$

$$f_{0 \rightarrow 0} \approx \frac{1}{2} \left[ 2\psi(1) - \psi(s+1) - \ln\left(\frac{s^2}{4}\right) \right] \quad (2.35)$$

$$f_{1 \rightarrow 0} \approx -\frac{1}{2} \frac{1}{\sqrt{s}} \quad (2.36)$$

Finally, the coulomb terms in (2.17) are simply

$$V_{0 \rightarrow 1} \approx -\frac{Ze^2}{L} \frac{\delta(-s-1+s')}{s+1} (C_2 C_2' + C_4 C_4') \quad (2.37)$$

$$V_{0 \rightarrow 0} = \frac{Ze^2}{L} \delta(s-s') \left[ 2\psi(1) - \psi(s+1) - \ln\left(\frac{s^2}{4}\right) \right] (C_2 C_2' + C_4 C_4') \quad (2.38)$$

$$V_{1 \rightarrow 0} = -\frac{Ze^2}{L} \frac{\delta(1-s-s')}{s} (C_2 C_2' + C_4 C_4') \quad (2.39)$$

## 2.4 The Coefficients $C_\mu$

The coefficients  $C_\mu$  are given by (Sokolov and Ternov 1968)

$$\begin{pmatrix} C_1 \\ C_2 \\ C_3 \\ C_4 \end{pmatrix} = \frac{1}{\sqrt{2K(K+k_0)}} \left[ \begin{pmatrix} K+k_0 \\ 0 \\ k_3 \\ \sqrt{4\gamma n} \end{pmatrix} D_1 + \begin{pmatrix} 0 \\ K+k_0 \\ \sqrt{4\gamma n} \\ -k_3 \end{pmatrix} D_{-1} \right] \quad (2.40)$$

where

$$K = E/\hbar c \quad (2.41)$$

$$k_0 = m_0 c/\hbar \quad (2.42)$$

$$k_3 = p_z/\hbar \quad (2.43)$$

$D_1=1$  and  $D_{-1}=0$  corresponds to the case where the electron's spin is parallel to the magnetic field.  $D_1=0$  and  $D_{-1}=1$  is the anti-parallel case. It is evident from equations (2.1) and (2.40) that a  $n=0$  ground state electron must have anti-parallel spin.

The appropriate spin summations indicated by equations (2.7), (2.16), and (2.17) are

$$\sum_{\mu}^{n=1} (H_{0 \rightarrow 1}, V_{1 \rightarrow 0}) \propto \sum_{\mu}^{n=1} \left( -\frac{p_z}{2m_0 c} C_1^{n=1} + C_3^{n=1} \right) \left( C_2^{n=1} - \frac{p_z}{2m_0 c} C_4^{n=1} \right) \quad (2.44)$$

$$\sim \frac{\hbar \delta^{1/2}}{m_0 c} \quad (2.45)$$

for the frequency and energy region being considered. Also

$$\sum_{\mu} (V_{0 \rightarrow \mu} H_{\mu \rightarrow 0}) \propto \frac{\hbar \delta^{1/2}}{m_0 c} \quad (2.46)$$

$$\sum_{\mu} (H_{0 \rightarrow \mu} V_{\mu \rightarrow 0}) \propto -\frac{p_z^0}{m_0 c} \quad (2.47)$$

$$\sum_{\mu} (V_{0 \rightarrow \mu} H_{\mu \rightarrow 0}) \propto -\frac{p_z^F}{m_0 c} \quad (2.48)$$

where  $p_z^0$  and  $p_z^F$  are the electron's initial and final momentum respectively.

## 2.5 The Energy Denominators

There are four possible energy denominators in equation (2.7) depending on whether the intermediate state is  $n=0$  or  $n=1$  and whether the photon is emitted before or after the coulomb interaction  $V_{ba}$ .

For  $n=0$

$$\begin{aligned} E_0 - E_I - \hbar\omega &\sim \frac{p\delta p}{m_0} - \hbar\omega \\ &\sim \left( \frac{p}{m_0 c} - 1 \right) \hbar\omega \\ &\sim -\hbar\omega \end{aligned} \quad (2.49)$$

where  $\delta p \sim \frac{\hbar\omega}{c}$  is a result of momentum conservation in  $H_{0 \rightarrow 0}$ .

Similarly, for  $n=0$

$$E_0 - E_{II} \sim \hbar\omega \quad (2.50)$$

For  $n=1$ , the results are simply

$$E_0 - E_I - \hbar\omega \sim E_0 - E_{II} \sim -\hbar\omega_c \quad (2.51)$$

where  $\omega_c$  is the gyro-frequency ( $\sim 10^{19} \text{ sec}^{-1}$  in  $10^{12}$  gauss).

## 2.6 The Matrix Element

Combining equations (2.7), (2.16), (2.37), (2.38), (2.39) and (2.45) through (2.51) gives the matrix element for the  $0 \rightarrow 0$  electron bremsstrahlung, namely

$$K_{F_0}^{0 \rightarrow 0} = e \frac{2\pi\hbar c}{k} \frac{Ze^2}{L} \left\{ \frac{1}{pc} \left[ -2\psi(1) - \psi(s+1) - 2 \ln \left( \frac{m_0 \omega}{2p\gamma^{1/2}} \right) \right] e_z \right. \\ \left. + \frac{\hbar\gamma^{1/2}}{m_0 c} \frac{1}{\hbar\omega_c} \left[ \frac{1}{\sqrt{s}} (ie_x + e_y) + \frac{1}{\sqrt{s+1}} (-ie_x + e_y) \right] \right\} \quad (2.52)$$

Rather than consider arbitrary photon angle and polarization, it is simpler and instructive to deal with propagation parallel and perpendicular to the magnetic field, and the two modes of propagation associated with each of these direction in a plasma.

For propagation along the magnetic field direction, there is (Bekefi 1965) an ordinary mode characterized by left-handed circular polarization, and an extraordinary mode with right-handed polarization. For perpendicular propagation both modes are linearly polarized. The ordinary wave's polarization vector is parallel to the magnetic field, whereas the extraordinary wave's vector is perpendicular to the magnetic field. The four polarization vectors are

$$\vec{e}(0|\theta=0) = \frac{1}{\sqrt{2}} (1, i, 0)$$

$$\vec{e}(X|\theta=0) = \frac{1}{\sqrt{2}} (1, -i, 0)$$

(2.53)

$$\vec{e}(0|\theta=\pi/2) = (0, 0, 1)$$

$$\vec{e}(X|\theta=\pi/2) = (1, 0, 0)$$

The resulting four matrix elements are

$$K(0|\theta=0) \approx \frac{2Ze^3}{L} \sqrt{\frac{\pi\hbar c}{\kappa}} \frac{\hbar\delta^{1/2}}{m_0 c} \frac{1}{\hbar\omega_c} \frac{1}{\sqrt{s}}$$

$$K(X|\theta=0) \approx \frac{2Ze^3}{L} \sqrt{\frac{\pi\hbar c}{\kappa}} \frac{\hbar\delta^{1/2}}{m_0 c} \frac{1}{\hbar\omega_c} \frac{1}{\sqrt{s+1}}$$

$$K(0|\theta=\pi/2) \approx \frac{Ze^3}{L} \sqrt{\frac{2\pi\hbar c}{\kappa}} \frac{1}{pc} \left[ -2\psi(1) - \psi(s+1) - 2\ln\left(\frac{m_0\omega}{2p\delta^{1/2}}\right) \right]$$

$$K(X|\theta=\pi/2) \approx \frac{Ze^3}{L} \sqrt{\frac{2\pi\hbar c}{\kappa}} \frac{\hbar\delta^{1/2}}{m_0 c} \frac{1}{\hbar\omega_c} \left( \frac{1}{\sqrt{s}} - \frac{1}{\sqrt{s+1}} \right)$$

(2.54)



## 2.7 Radiation Rates

The density of final states  $\rho_F$  is given by

$$\rho_F = \rho^e \rho^\gamma d\kappa \quad (2.55)$$

where  $\rho^\gamma$  is the usual photon number density, i.e.

$$\rho^\gamma = \frac{\kappa^2 d\Omega_\gamma}{(2\pi)^3} \quad (2.56)$$

The electron number density however, is not the usual three-dimensional form as in ordinary bremsstrahlung. The momentum  $p_z$  along the magnetic field has discrete values for finite  $L$ .

$$p_z / \hbar = 2\pi n_3 / L \quad (n_3 = 0, \pm 1, \pm 2 \dots) \quad (2.57)$$

$$E = p_{zm}^2$$

$$\rho^e = \frac{dn_3}{dE} = \frac{Lm}{2\pi\hbar p_z} \quad (2.58)$$

$$\rho_F = \left( \frac{Lm}{2\pi\hbar} \right) \frac{1}{p_z} \frac{\kappa^2 d\kappa d\Omega_\gamma}{(2\pi)^3} \quad (2.59)$$

The differential radiation rate (i.e. emissivity) is given by

$$\frac{dI}{d\omega d\Omega_\gamma} = \frac{W \hbar \omega}{d\omega d\Omega_\gamma} \quad (2.60)$$

Therefore, combining equations (2.6), (2.54), (2.59), and (2.60) gives the four radiation rates

$$\frac{dI}{d\omega d\Omega_\gamma} (0|\theta=0) \approx \frac{Z^2 e^6}{2\pi^2 m_0 c^3 L} \frac{\omega^2}{\omega_c^2} \frac{\gamma}{s} \frac{1}{p_z}$$

$$\frac{dI}{d\omega d\Omega_\gamma} (X|\theta=0) \approx \frac{Z^2 e^6}{2\pi^2 m_0 c^3 L} \frac{\omega^2}{\omega_c^2} \frac{\gamma}{s+1} \frac{1}{p_z}$$

$$\frac{dI}{d\omega d\Omega_\gamma} (0|\theta=\pi/2) \approx \frac{Z^2 e^6}{4\pi^2 c^3 L} \frac{\omega^2}{p_z} \left[ -2\psi(1) - \psi(s+1) - 2\ln\left(\frac{m_0 \omega}{2p_z \gamma^{1/2}}\right) \right]^2$$

$$\frac{dI}{d\omega d\Omega_\gamma} (X|\theta=\pi/2) \approx \frac{Z^2 e^6}{4\pi^2 m_0 c^3 L} \frac{\omega^2}{\omega_c^2} \frac{\gamma}{p_z} \left( \frac{1}{\sqrt{s}} - \frac{1}{\sqrt{s+1}} \right)^2$$

(2.61)

Recalling that the trajectory center is essentially  $\sqrt{s_0} = b$  and moreover simply represents the impact parameter for the bremsstrahlung process, the  $\theta=0$  emissivities can be written in the form

$$\frac{dI}{d\omega d\Omega_\gamma} (\theta=0) \approx A \frac{\omega^2}{\omega_c^2} \frac{1}{p_z} \frac{1}{b^2} \quad (2.62)$$

where

$$A = \frac{Z^2 e^6}{2\pi^2 m_0 c^3 L} \quad (2.63)$$

This result differs from that of ordinary bremsstrahlung (i.e. non-magnetic) as derived in classical electrodynamics (Jackson 1965), by a factor of  $\frac{\omega^2}{\omega_c^2}$ . This is the damping factor one expects for scattering by a bound oscillator whose resonant frequency is the gyro-frequency (Heitler 1954). Thus a magnetic field of about  $10^{12}$  gauss reduces the forward emission by a factor of  $\sim 10^{22}$  for  $\omega \sim 10^8$   $\text{sec}^{-1}$ .

Using the approximation

$$\psi(s+1) \sim \ln s \quad (2.64)$$

yields the result

$$\frac{dI}{d\omega d\Omega_\gamma} (0|\theta=\pi/2) \approx \frac{Z^2 e^6}{\pi^2 c^3 L} \frac{\omega^2}{P_z^3} \ln^2 \left( \frac{P_z}{m_0 \omega b} \right) \quad (2.65)$$

which is, not surprisingly, independent of the magnetic field. For  $E \sim 1$  kev,  $\omega \sim 10^8$   $\text{sec}^{-1}$ ,  $B \sim 10^{12}$  gauss, and  $b \sim 1$  Å, it is a factor of  $\sim 10^6$  larger than the  $\theta=0$  emissivities.

## 2.8 Summations Over The Radial Quantum Number 's'

The radiation rates given in equations (2.61) are for a single electron-ion interaction and for a particular quantum number 's'. If the electron is traversing a region where the ion density is  $N_i$ , an appropriate summation over 's' must be made. The net radiation rate is then

$$\left\langle \frac{dI}{d\omega d\Omega} \right\rangle = \sum_s \left( \frac{dI}{d\omega d\Omega} \right)_s N(s) \quad (2.66)$$

where 
$$N(s) \approx N_i L 2\pi b \Delta r = N_i L \frac{\pi}{\gamma} \quad (2.67)$$

since 
$$b \approx \sqrt{\frac{2}{\gamma}}$$

The four pertinent summations are

$$\begin{aligned} & \sum_s \frac{1}{s} \\ & \sum_s \frac{1}{s+1} \\ & \sum_s \left[ -2\psi(1) - \psi(s+1) - 2 \ln \left( \frac{m_e \omega}{2 p_z \gamma^2 b} \right) \right]^2 \\ & \sum_s \left( \frac{1}{\sqrt{s}} - \frac{1}{\sqrt{s+1}} \right)^2 \end{aligned} \quad (2.68)$$

Approximating these summations by integrations gives

$$\sum_s \frac{1}{s} \sim \int_{s_{\min}}^{s_{\max}} \frac{ds}{s} = \ln \left( \frac{s_{\max}}{s_{\min}} \right) \quad (2.69)$$

$$\sum_s \frac{1}{s+1} \sim \int_{s_{\min}}^{s_{\max}} \frac{ds}{s+1} = \ln \left( \frac{s_{\max}+1}{s_{\min}+1} \right) \quad (2.70)$$

$$\begin{aligned} \sum_s \left[ -2\psi(1) - \psi(s+1) - 2 \ln \left( \frac{m_0 \omega}{2 p_z \gamma^{1/2}} \right) \right]^2 &\sim \sum_s \ln^2 \left( \frac{m_0^2 \omega^2 s}{p_z^2 \gamma} \right) \\ &\sim \int_{s_{\min}}^{s_{\max}} \ln^2 \left( \frac{m_0^2 \omega^2 s}{p_z^2 \gamma} \right) ds \\ &= \left[ s \ln^2 \left( \frac{m_0^2 \omega^2 s}{p_z^2 \gamma} \right) - 2s \ln \left( \frac{m_0^2 \omega^2 s}{p_z^2 \gamma} \right) + 2s \right]_{s_{\min}}^{s_{\max}} \end{aligned} \quad (2.71)$$

$$\sum_s \left( \frac{1}{\sqrt{s}} - \frac{1}{\sqrt{s+1}} \right)^2 \sim \int_{s_{\min}}^{s_{\max}} \left( \frac{1}{\sqrt{s}} - \frac{1}{\sqrt{s+1}} \right)^2 ds = \left\{ 2 \ln \left[ \frac{(s^2+s)^{1/2}}{2(s^2+s)+2s+1} \right] \right\}_{s_{\min}}^{s_{\max}} \quad (2.72)$$

The net radiation rates are therefore given by

$$\left\langle \frac{dI}{d\omega d\Omega} (0|\theta=0) \right\rangle = \frac{Z^2 e^6}{2\pi m_0 c^3} N_i \frac{\omega^2}{\omega_c^2} \frac{1}{p_z} \left[ \ln s \right]_{s_{\min}}^{s_{\max}}$$

$$\left\langle \frac{dI}{d\omega d\Omega} (x|\theta=0) \right\rangle = \frac{Z^2 e^6}{2\pi m_0 c^3} N_i \frac{\omega^2}{\omega_c^2} \frac{1}{p_z} \left[ \ln(s+1) \right]_{s_{\min}}^{s_{\max}}$$

$$\left\langle \frac{dI}{d\omega d\Omega} (0 | \theta = \frac{\pi}{2}) \right\rangle \approx \frac{Z^2 e^6}{4\pi c^3} N_i \frac{\omega^2}{p_z^3} \frac{1}{\gamma} \left[ s \ln^2 \left( \frac{m_0^2 \omega^2 s}{p^2 \gamma} \right) - 2s \left( \frac{m_0^2 \omega^2 s}{p^2 \gamma} \right) + 2s \right]_{s_{\min}}^{s_{\max}}$$

$$\left\langle \frac{dI}{d\omega d\Omega} (x | \theta = \frac{\pi}{2}) \right\rangle \approx \frac{Z^2 e^6}{2\pi m_0 c^3} N_i \frac{\omega^2}{\omega_c^2} \frac{1}{p_z} \left\{ \ln \left[ \frac{(s^2 + s)^{1/2}}{2(s^2 + s)^{1/2} + 2s + 1} \right] \right\}_{s_{\min}}^{s_{\max}} \quad (2.73)$$

Since  $b \sim \sqrt{s/\gamma}$

$$[\ln s]_{s_{\min}}^{s_{\max}} = 2 \ln \left( \frac{b_{\max}}{b_{\min}} \right) \quad (2.74)$$

i.e. the familiar bremsstrahlung logarithmic factor (Jackson 1965).

The usual quantum-mechanical expression for  $b_{\min}$  is

$$b_{\min} \sim \frac{\hbar}{m v} \quad (2.75)$$

$$\sim 10^{-9} \text{ cm} \quad E \sim 1 \text{ kev}$$

$$\sim \sqrt{1/\gamma} \quad B \sim 10^{12} \text{ gauss}$$

which implies  $s_{\min} \sim 1$

The choice of  $b_{\max}$  depends on screening conditions etc. Possible values are  $\frac{v}{\omega}$  (no screening) to  $\sim 1 \text{ \AA}$  (atomic screening). In neutron star atmospheres, for example, the latter case would seem more appropriate considering their high density ( $\sim 1 \text{ gm/cm}^3$ ).

For  $E \sim 1 \text{ kev}$ ,  $B \sim 10^{12} \text{ gauss}$ , and  $\omega \sim 10^8 \text{ sec}^{-1}$

$$b_{\max} \sim \frac{v}{\omega} \Rightarrow s_{\max} \sim \gamma \frac{v^2}{\omega^2} \sim 10^{21}$$

$$r_{\max} \sim 1 \text{ \AA} \Rightarrow s_{\max} \sim 10^3$$

i.e. both cases lead to high values of  $s_{\max}$ .

Withholding a factor

$$B = \frac{Z^2 e^6}{2\pi m_e c^3} N_i \frac{\omega^2}{\omega_c^2} \frac{1}{P_z} \quad (2.76)$$

the radiation rates can be tabulated as follows:

$$E \sim 1 \text{ keV}$$

$$\omega \sim 10^8 \text{ sec}^{-1}$$

$$\hbar \omega \sim 10^{12} \text{ yewss}$$

$$s_{\max} \sim 10^{21}$$

$$s_{\max} \sim 10^3$$

$$\frac{1}{B} \left\langle \frac{dI}{d\omega d\Omega} (0 | \theta = 0) \right\rangle$$

$$\sim 48$$

$$\sim 7$$

$$\frac{1}{B} \left\langle \frac{dI}{d\omega d\Omega} (X | \theta = 0) \right\rangle$$

$$\sim 48$$

$$\sim 6$$

$$\frac{1}{B} \left\langle \frac{dI}{d\omega d\Omega} (0 | \theta = \frac{\pi}{2}) \right\rangle$$

$$\sim 10^{22}$$

$$\sim 10^7$$

$$\frac{1}{B} \left\langle \frac{dI}{d\omega d\Omega} (X | \theta = \frac{\pi}{2}) \right\rangle$$

$$\sim 10^{-2}$$

$$\sim 10^{-2}$$

## 2.9 Some Polarization Aspects

Two circularly polarized components propagate in the  $\theta=0$  direction. The question arises as to what the net polarization is. For sufficiently low densities their indices of refraction are essentially the same and the degree of polarization  $p$  is simply

$$p = \frac{I_o - I_x}{I_o + I_x} \quad (2.77)$$

From equations (2.73)

$$I_o \propto \ln(s_{\max})$$

$$I_x \propto \ln(s_{\max} + 1)$$

Therefore

$$p \approx \frac{\ln 2}{2 \ln(s_{\max}) - \ln 2} \quad (2.78)$$

i.e.

$$s_{\max} \sim 10^{21} \Rightarrow p \approx .7 \%$$

$$s_{\max} \sim 10^3 \Rightarrow p \approx 11 \%$$



### Chapter 3

#### CLASSICAL CALCULATION

The equation of motion of an electron moving in a coulomb field and a magnetic field is

$$m \frac{d^2 \vec{r}}{dt^2} = - \frac{Ze^2}{r^3} \vec{r} - \frac{e}{c} \vec{v} \times \vec{B} \quad (3.1)$$

Consider a dimensionless vector  $\vec{a}$ , related to the electron's position vector  $\vec{r}$ , as given by

$$\vec{a} = \frac{\vec{r}}{b} = \frac{\vec{b}}{b} + \alpha_z^{(0)} + \delta \vec{a}_z^{(1)} + \epsilon \vec{a}_1^{(1)} + \delta^2 \vec{a}_z^{(2)} \quad (3.2)$$

where  $\vec{b}$  is perpendicular to the electron's trajectory along the z-axis, and is equal in magnitude to the impact parameter  $b$ .  $\delta$  and  $\epsilon$  are infinitesimals related to the higher order terms of  $\vec{a}$ .

A dimensionless time variable  $\tau$  is also defined.

$$\tau = \frac{tv_0}{b} \quad (3.3)$$

Putting  $\vec{a}$  and  $\tau$  in the equation of motion gives

$$\ddot{\vec{a}} = - \frac{Ze^2 \vec{a}}{b^3 m v_0^2} - \frac{eb\vec{v}}{mc v_0} (\dot{\vec{a}} \times \hat{e}_z) \quad (3.4)$$

where

$$\bullet \equiv \frac{d}{d\tau}$$

Now, for  $b \sim 1 \text{ \AA}$ ,  $v_0 \sim 10^9 \text{ cm/sec}$ , and  $\mathcal{H} \sim 10^{12} \text{ gauss}$ ,

$$\frac{Ze^2}{b\mu_0^2} \sim 10^{-2} \ll 1 \quad (3.5)$$

$$\frac{e\mathcal{H}b}{mcv_0} \sim 10^2 \gg 1 \quad (3.6)$$

Let

$$\delta = \frac{Ze^2}{b\mu_0^2} \quad (3.7)$$

and

$$\epsilon^{-1} = \frac{e\mathcal{H}b}{mcv_0} \quad (3.8)$$

Then equation (3.4) becomes

$$\ddot{\vec{a}} = -\delta \frac{\vec{a}}{a^3} - \epsilon^{-1} (\dot{\vec{a}} \times \hat{e}_z) \quad (3.9)$$

Substituting for  $\vec{a}$  with equation (3.2) and comparing like orders gives

$$\begin{aligned} \ddot{a}_z^{(0)} &= 0 \\ \ddot{a}_z^{(1)} &= -\frac{a_z^{(0)}}{a^3} \end{aligned} \quad (3.10)$$

$$\begin{aligned} \ddot{a}_\perp^{(1)} &= 0 \\ \ddot{a}_\perp^{(2)} &= -\frac{\delta}{\epsilon} \frac{\hat{e}_z \times \vec{b}}{a^3 b} \end{aligned}$$

Now

$$\alpha = \frac{\lambda}{b} = \sqrt{1 + \tau^2} \quad (3.11)$$

and

$$\alpha_z^{(6)} = \frac{vt}{b} = \tau$$

Therefore

$$\ddot{\vec{a}}_z^{(1)} = - \frac{\tau}{(1 + \tau^2)^{3/2}} \quad (3.12)$$

$$\dot{\vec{a}}_{\perp}^{(2)} = - \frac{\oint \hat{\vec{e}}_z \times \hat{\vec{b}}}{\epsilon (1 + \tau^2)^{3/2}} \quad (3.13)$$

Thus the parallel acceleration is a lower order effect than the perpendicular acceleration.

The energy radiated in the collision is given by (Jackson 1965)

$$\begin{aligned} \frac{dE}{d\omega d\Omega} &= \frac{e^2}{4\pi^2 c} \left| \int_{-\infty}^{\infty} \vec{n} \times \left( \vec{n} \times \frac{\dot{\vec{a}}}{c} \right) e^{i\omega t} dt \right|^2 \\ &= \frac{e^2 v^2}{4\pi^2 c^3 b} \left| \int_{-\infty}^{\infty} \vec{n} \times (\vec{n} \times \ddot{\vec{a}}) e^{\frac{i\omega b}{v} \tau} d\tau \right|^2 \quad (3.14) \end{aligned}$$

Combining equations (3.12), (3.13), (3.14), 3.7), and (3.8) gives

$$\frac{dE}{d\omega d\Omega} (\theta=0) = \frac{Z^2 e^6}{4\pi^2 m c^3} \frac{\omega^2}{\omega_e^2} \frac{1}{b^2} \frac{1}{p} \frac{1}{v} \quad (3.15)$$

$$\frac{dE}{d\omega d\Omega} (\theta = \pi/2) = \frac{Z^2 e^6 m}{4\pi^2 c^3} \frac{\omega^2}{p^3} \ln^2\left(\frac{v}{\omega b}\right) \frac{1}{v} \quad (3.16)$$

The radiation rates are obtained by simply dividing these results by the effective collision time ( $\sim 1/v$ ).

$$\frac{dI}{d\omega d\Omega} (\theta=0) = \frac{Z^2 e^6}{4\pi^2 m c^3 L} \frac{\omega^2}{\omega_c^2} \frac{1}{b^2} \frac{1}{p} \quad (3.17)$$

$$\frac{dI}{d\omega d\Omega} (\theta=\pi/2) = \frac{Z^2 e^6 m}{4\pi^2 c^3 L} \frac{\omega^2}{p^3} \ln^2\left(\frac{v}{\omega b}\right) \quad (3.18)$$

These emissivities correlate with the quantum-mechanical results given in equation (2.61) since

$$\Psi(s+1) \sim \ln s \quad (3.19)$$

and

$$b \approx \sqrt{s/\gamma}$$

$$\text{i.e.} \quad \left[ -2\Psi(1) - \Psi(s+1) - 2\ln\left(\frac{m_0 \omega}{2p\gamma^{1/2}}\right) \right]^2 \approx 4 \ln^2\left(\frac{v\gamma^{1/2}}{\omega s^{1/2}}\right)$$

$$\approx 4 \ln^2\left(\frac{v}{\omega b}\right) \quad (3.20)$$

## Chapter 4

### CONCLUSIONS AND DISCUSSION

The non-relativistic bremsstrahlung radiation rate of an electron interacting with ions in an intense magnetic field exhibits :

- (1) a  $1/p_z$  dependence due to the essentially one-dimensional momentum space,
- (2) a  $\frac{\omega^2}{\omega_c^2}$  attenuation in the  $\theta=0$  direction relative to the non-magnetic bremsstrahlung due to the "binding" effect of the magnetic field,
- (3) a  $\theta=\pi/2$  emissivity larger than the  $\theta=0$  emissivity for the same reason as (2),
- (4) a net left-handed circular polarization in the  $\theta=0$  direction due to the differing mode emissivities,
- (5) a momentum dependence (i.e.  $1/p_z$ ) that satisfies the condition for coherent amplification (i.e.  $\frac{\partial}{\partial p} \left( \frac{I}{p} \right) < 0$ ).

# Appendix 1

## AMPLIFICATION CONDITION

Aside from positive factors, the absorption coefficient for one-dimensional electron bremsstrahlung is (Chiu and Camuto 1970)

$$\alpha_{\omega} \sim - C(\omega, \theta) \int_{-\infty}^{\infty} [f(p') - f(p)] W(p, p') dp$$

$$C(\omega, \theta) > 0 \quad (A1.1)$$

where  $W(p, p')$  is the transition probability rate  $p \rightarrow p'$ , and  $f(p)$  is the one-dimensional electron momentum distribution.

Using the approximation

$$f(p') \sim f(p) + \frac{\partial f}{\partial p} |\Delta p| \quad (A1.2)$$

gives

$$\alpha_{\omega} \sim - C(\omega, \theta) \int_{-\infty}^{\infty} \left( \frac{\partial f}{\partial p} |\Delta p| \right) W(p, p') dp \quad (A1.3)$$

Since  $f(\pm\infty) = 0$ , partially integrating this expression gives

$$\alpha_{\omega} \sim C(\omega, \theta) \int_{-\infty}^{\infty} f(p) \frac{\partial}{\partial p} (W(p, p') |\Delta p|) dp \quad (A1.4)$$

Since  $f(p) > 0$ , a necessary condition for  $\alpha_\omega$  to be negative is

$$\frac{\partial}{\partial p} \left( w(p, p') |\Delta p| \right) < 0 \quad (A1.5)$$

Simon and Strange (1969) made the mistake of putting

$$|\Delta p| \sim \frac{\hbar \omega}{c}$$

(i.e. momentum conservation) rather than the energy conserving result  
(2.31)

$$|\Delta p| \sim \frac{m \hbar \omega}{p}$$

Thus the amplification condition is (Chiu and Canuto 1970)

$$\frac{\partial}{\partial p} \left( \frac{w(p, p')}{p} \right) < 0 \quad (A1.6)$$

## Appendix 2

### THE RADIATION TERM

$$H_{nsp_z \rightarrow n's'p_z'} = -e \sqrt{\frac{2\pi\hbar c}{\kappa}} \vec{\kappa} \cdot \vec{e} \quad (A2.1)$$

where

$$\vec{\kappa} = \int \Psi_{n's'p_z'}^* e^{-i\vec{\kappa} \cdot \vec{r}} \vec{\kappa} \Psi_{nsp_z} d^3x \quad (A2.2)$$

$\vec{\kappa} \equiv$  dirac matrices

$\vec{e} \equiv$  photon polarization vector

Because of the axial symmetry of the external magnetic field, let the photon's propagation vector  $\vec{\kappa}$  be parallel to the YZ plane.

Then

$$\kappa_x = 0 \quad \kappa_y = \kappa \sin \Theta \quad \kappa_z = \kappa \cos \Theta \quad (A2.3)$$

and

$$\vec{\kappa} \cdot \vec{r} = \kappa r \sin \Theta \sin \phi + \kappa z \cos \Theta \quad (A2.4)$$

where  $(r, \phi, z)$  are the electron's cylindrical coordinates.

The electron's wave function is of the form

$$\Psi_{nsp_z} = \frac{e^{\frac{ip_z z}{\hbar}}}{\sqrt{L}} \frac{e^{i(l-1/2)\phi}}{\sqrt{2\pi}} f(\phi, r) \quad (A2.5)$$

Therefore



$$\vec{a} = \frac{1}{L} \int_{-L/2}^{L/2} e^{-\frac{i}{k} (p_z' + k \kappa \cos \Theta - p_z) z} dz \frac{1}{2\pi} \int_0^{2\pi} d\phi \int_0^{\infty} r dr e^{-ikr \sin \Theta \sin \phi + i(l-l')\phi} \frac{f' r^2}{f} \quad (A2.6)$$

Applying the integral relations (Sokolov and Ternov 1968)

$$\frac{1}{L} \int_{-L/2}^{L/2} dz e^{-\frac{i}{k} (p_z' + k \kappa \cos \Theta - p_z) z} = \delta(p_z' + k \kappa \cos \Theta - p_z) \quad (A2.7)$$

$$\frac{1}{2\pi} \int_0^{2\pi} d\phi e^{-ikr \sin \Theta \sin \phi + i(l-l')\phi} = J_{l-l'}(\kappa r \sin \Theta) \quad (A2.8)$$

$$\int_0^{\infty} J_{l-l'}(2\sqrt{x}\rho) I_{n',s'}(\rho) I_{n,s}(\rho) d\rho = I_{n,n'}(\chi) I_{s,s'}(\chi) \quad (A2.9)$$

where

$$\rho = \delta r^2$$

and

$$\chi = \frac{\kappa^2 \sin \Theta}{4\delta}$$

and as given in equation (2.1)

$$f = \sqrt{2\delta} \begin{pmatrix} c_1 e^{-i\phi/2} I_{n-1,s}(e) \\ i c_2 e^{i\phi/2} I_{n,s}(e) \\ c_3 e^{-i\phi/2} I_{n-1,s}(e) \\ i c_4 e^{i\phi/2} I_{n,s}(e) \end{pmatrix}$$

yields the result

$$\begin{pmatrix} \bar{a}_x \\ \bar{a}_y \end{pmatrix} = \delta(p_z' + \hbar k \omega_3 \Theta - p_z) \left[ \begin{pmatrix} i \\ 1 \end{pmatrix} (C_1' C_4 + C_3' C_2) I_{n, n'-1} + \begin{pmatrix} -i \\ 1 \end{pmatrix} (C_4' C_1 + C_2' C_3) I_{n-1, n'} \right] I_{s, s'}$$

$$\bar{a}_z = \delta(p_z' + \hbar k \omega_3 \Theta - p_z) \left[ (C_1' C_3 + C_3' C_1) I_{n-1, n'-1} - (C_4' C_2 + C_2' C_4) I_{n, n'} \right] I_{s, s'}$$

where  $\chi$  is the argument of the Laguerre functions.

REFERENCES

- Bekefi, G. 1965, Radiation Processes in Plasmas (New York: John Wiley & Sons, Inc.).
- Cameron, A. C. W. 1970, Ann. Rev. Astron. and Astrophys., 8, 179.
- Canuto, V., Chiu, H. Y., and Fasso-Camuto, L. 1969, Phys. Rev., 185, 1607.
- Chiu, H. Y., and Canuto, V. 1969, Phys. Rev. Ltrs., 22, 415.
- . 1970, Nature, 225, 1230.
- Gold, T. 1968, Nature, 218, 731.
- Gradshteyn, I. S., and Ryzhik, I. M. 1965, Table of Integrals, Series, and Products (New York: Academic Press).
- Gunn, J., and Ostriker, J. 1969, Ap. J., 157, 1395.
- Heitler, W. 1954, Quantum Theory of Radiation (Oxford: Oxford Press).
- Hewish, A., et al. 1968, Nature, 217, 709.
- Jackson, J. D. 1965, Classical Electrodynamics (New York: John Wiley & Sons, Inc.).
- Simon, M., and Strange, D. L. P. 1969, Nature, 224, 49.
- Sokolov, A. A., and Ternov, I. M. 1968, Synchrotron Radiation (New York: Pergamon Press).

Part II

ATOMS IN AN INTENSE MAGNETIC FIELD

## Chapter 5

### INTRODUCTION

In part I of this thesis, consideration was given to electron bremsstrahlung in an intense magnetic field of  $\sim 10^{12}$  gauss. In part II electrons bound in atoms are studied to see what effect such a strong magnetic field has on

- (a) the electron energy levels and orbits of hydrogen,
- (b) the ionization fraction of a hydrogen plasma, and
- (c) the size and electron distribution of high Z atoms.

Topics (a) and (c) have been investigated independently by other workers. Cohen et al. (1970) have looked at the binding energies of low Z atoms by making a Hartree calculation. Canuto and Kelly have computed the hydrogen energy levels via perturbation theory and numerical methods. Kadomstev (1970) looked at high Z atoms in the Thomas-Fermi approximation.

These studies, along with my own, represent a preliminary effort to see what role atomic physics might play in a neutron star atmosphere. Investigations have since expanded to include many related aspects of neutron star matter such as electrical conductivity, bulk magnetic moment, etc.

In the following chapter, hydrogen is dealt with from four viewpoints:

(1) A "Bohr" picture.

A nice place to start is with a simple Bohr hydrogen model, namely an electron in a circular orbit about a proton. To this situation is added a magnetic field  $\vec{H}$  perpendicular to the orbital plane. Modifications are made to the equations of motion and new quantized orbit radii  $r_l$  and energy levels  $E_l$  are obtained. It becomes immediately apparent from these results that  $E_l \geq 0$  (i.e. no bound states) for  $H \geq 4 \times 10^9$  gauss. Thus, in order to get a bound state when  $H \geq 4 \times 10^9$  gauss, the electron motion must be along  $\vec{H}$ , not perpendicular to it. This is the "one-dimensional" aspect also discovered in part I in regard to electron motion in such magnetic fields.

(2) The "one-dimensional" hydrogen atom.

The need for one-dimensional motion, as indicated by the "Bohr" picture, is immediately applied by considering a model where the electron is constrained to oscillate back and forth on a magnetic field line. This means solving the Schroedinger equation for a potential like

$$V(z) = \frac{-e^2}{\sqrt{z^2 + b^2}} \quad (5.1)$$

It is easier to make use of solutions already available, namely those for

$$V(z) = \frac{-e^2}{|z|} \quad (5.2)$$

and 
$$V(z) = \frac{-e^2}{|z| + b} \quad (5.3)$$

The latter potential, sometimes referred to as the truncated coulomb potential, is a reasonable approximation of (5.1) and therefore is used to obtain the energy levels of the model.

### (3) Variational Calculation #1.

An improvement on (2) is the use of

$$V(z) = \frac{-e^2}{\sqrt{z^2 + b_s^2}} \quad (5.4)$$

instead of the truncated coulomb potential approximation. This is done by using the technique of variational calculus. The trial wave function adopted for this computation is

$$f_s(z) = \left(\frac{A_s}{a_0}\right)^{1/2} e^{-\frac{A_s |z|}{a_0}} \quad (5.5)$$

i.e. an appropriate hydrogenic form.

### (4) Variational Calculation #2.

Finally, a still further improvement on (2) and (3) is the use of a three-dimensional potential and wave function.

$$V(r, z) = \frac{-e^2}{\sqrt{r^2 + z^2}} \quad (5.6)$$

$$\psi_s(r, z) = \sqrt{2s} \left(\frac{e^{-r} e^s}{s!}\right)^{1/2} \left(\frac{\alpha_s}{\sqrt{\pi}}\right)^{1/2} e^{-\frac{\alpha_s^2 z^2}{2}} \quad (5.7)$$

$$\rho = \gamma n^2 \quad (5.8)$$

$$\gamma = \frac{e \hbar}{2 \hbar c} \quad (5.9)$$

The trial wave function now combines the radial part of the free electron wave function in a magnetic field with a Gaussian envelope.

These four progressively better model computations give a quantitative and qualitative picture of hydrogen in a magnetic field of  $\sim 10^{12}$  gauss - the electron oscillating back and forth in a cylindrical shell, the two sets of energy levels, and a ground state binding energy of  $\sim 200$  ev.

With this information in hand, a plasma of such hydrogen is considered, as it might exist in a neutron star atmosphere. The Saha equation is modified to allow for "one-dimensional" statistics, the "new" energy levels, and the "higher" ionization potential. The ionization fraction is then obtained for a temperature of  $\sim 10^6$  °K.

Finally, multi-electron atoms are investigated briefly using the Thomas-Fermi approximation.



## Chapter 6

### HYDROGEN

#### 6.1 A "Bohr" Picture

A simple model for a hydrogen atom in a homogeneous magnetic field is the "Bohr" picture suggested by Camuto and Kelly, namely an electron orbiting a stationary proton with the plane of the orbit perpendicular to the magnetic field direction. No kinetic energy along the magnetic field is allowed.

The equations governing this motion are (Camuto and Kelly)

$$\frac{mv^2}{r} = \frac{e\hbar v}{c} + \frac{e^2}{r^2}$$

$$E = \frac{1}{2} mv^2 - \frac{e^2}{r} \quad (6.1)$$

$$mvr = (l+1)\hbar \quad l = 0, 1, 2, \dots$$

These equations give discrete radius and energy values.

$$r_l = \frac{1}{4(l+1)a_0\gamma} \left( \sqrt{1 + 8(l+1)^3 a_0^2 \gamma} - 1 \right) \quad (6.2)$$

$$E_l = \frac{1}{2} (l+1)\hbar\omega_c - \frac{e^2}{2r_l}$$

where  $a_0$  is the "ordinary" Bohr radius and

$$\gamma = \frac{e\hbar}{2\hbar c} \quad \omega_c = \frac{e\hbar}{mc} \quad (6.3)$$

as before.

In the limit of zero magnetic field, the expressions for  $r_l$  and  $E_l$  reduce to the expected classical Bohr results.

$$\lim_{\hbar \rightarrow 0} r_l = (l+1)^2 a_0 \quad (6.4)$$

$$\lim_{\hbar \rightarrow 0} E_l = -\frac{e^2}{2(l+1)^2 a_0}$$

The same classical results can also be obtained by letting the proton charge get very large. For a nucleus of charge  $Ze$  the equations (6.2) need be modified only slightly to give

$$r_l = \frac{1}{4(l+1)a_0\gamma} \left( \sqrt{Z + 8(l+1)^3 a_0^2 \gamma} - Z \right) \quad (6.5)$$

$$E_l = \frac{1}{2}(l+1)\hbar\omega_c - \frac{Ze^2}{2r_l}$$

For large  $Z$

$$r_l \rightarrow \frac{a_0(l+1)^2}{Z}$$

$$E_l \rightarrow -\frac{Z^2 e^2}{2(\ell+1)^2 a_0} \quad (6.6)$$

i.e. the expected classical Bohr results for a hydrogenic atom with a nucleus having a charge  $Ze$ .

Both these limits (i.e. small  $\vec{H}$ , large  $Z$ ) simply elevate the Coulomb potential to complete dominance thereby bringing back the familiar Bohr atom results. Of more interest here is the region of large  $\vec{H}$ . For large  $\vec{H}$

$$n_l \rightarrow \sqrt{\frac{(\ell+1)}{2\gamma}} \quad (6.7)$$

$$E_l \rightarrow \frac{1}{2}(\ell+1)\hbar\omega_c$$

These limits are the usual parameters of a free electron in a magnetic field, the electron having no motion along the field. From section 2.1

$$R = \sqrt{n/\gamma} \quad (6.8)$$

$$E = n\hbar\omega_c$$

It is evident from all these limiting cases that positive as well as negative energy states are possible. Above a certain magnetic field  $E_l > 0$  denoting an unbound state. This critical magnetic field  $H_l^c$  is easily obtained from the condition  $E_l = 0$  and equations (6.2).

$$H_l^c = \frac{m^2 e^3 c}{\hbar^3 (\ell+1)^3} = \frac{4 \times 10^9}{(\ell+1)^3} \text{ gauss} \quad (6.9)$$

Thus above  $H \sim 4 \times 10^9$  gauss, this "Bohr" picture doesn't give bound states. For stronger magnetic fields the magnetic kinetic energy is simply larger than the coulomb binding energy (see Fig. 1). Therefore, in order to get a bound state when  $H \sim 10^{12}$  gauss, the motion of the electron must be mostly along the magnetic field direction. This immediately suggests the "n=0" ground state electron discussed in part I. The coulomb field could force such an electron to oscillate back and forth along a magnetic field line. It is just such a model that is discussed in the next three sections.

## 6.2 Truncated Coulomb Potential

Another simplistic picture is that of an electron constrained to oscillate back and forth on a magnetic field line near a stationary proton. A quick estimate of the resultant energy levels is obtained by using the truncated coulomb potential

$$V(z) = \frac{-e^2}{|z| + b} \quad (6.10)$$

with a suitable choice for  $b$ . The Schroedinger equation for the system is

$$-\frac{\hbar^2}{2m} \frac{d^2 \psi_N}{dz^2} - \frac{e^2 \psi_N}{|z| + b} = E_N \psi_N \quad (6.11)$$

and has been solved for  $b \ll a_0$  (Haines and Roberts 1969).

$$E_0 = -\frac{\hbar^2}{2ma_0^2} \left[ 2 \ln(a_0/b) \right]^2 \quad \text{ground state}$$

$$E_N = -\frac{\hbar^2}{2ma_0^2 N^2} \times \begin{cases} 1 - \frac{4b}{Na_0} & \text{odd parity} \\ 1 - \frac{2}{N \ln(a_0/b)} & \text{even parity} \end{cases} \quad (6.12)$$

N 1,2,3....

A reasonable choice for  $\psi$  can be arrived at by considering the radial part of the  $n=0$  electron wave function.

$$\Psi_s(\rho) \sim \sqrt{2\gamma} \left( \frac{e^{-\rho} \rho^s}{s!} \right)^{1/2} \quad (6.13)$$

The root mean square radial distance is

$$\begin{aligned} \langle r^2 \rangle_s^{1/2} &= \int_0^\infty \frac{e^{-\rho} \rho^s}{s!} \frac{\rho}{\gamma} d\rho^{1/2} \\ &= \sqrt{\frac{s+1}{\gamma}} \end{aligned} \quad (6.14)$$

i.e. let 
$$\psi_s = \langle r^2 \rangle_s^{1/2} = \sqrt{\frac{s+1}{\gamma}} \quad (6.15)$$

The quantum number 's' is now non-degenerate and adds "structure" to the energy levels of hydrogen.

$$\begin{aligned} E_{0,s} &\approx -\frac{\hbar^2}{2ma_0^2} \left[ \ln \left( \frac{\gamma a_0^2}{s+1} \right) \right]^2 \\ E_{N,s} &= -\frac{\hbar^2}{2ma_0^2 N^2} \times \begin{cases} 1 - \frac{4}{N} \sqrt{\frac{s+1}{\gamma a_0^2}} \\ 1 - \frac{4}{N \ln \left( \frac{\gamma a_0^2}{s+1} \right)} \end{cases} \end{aligned} \quad (6.16)$$

For  $N \sim 10^{12}$  gauss

$$\gamma a_0^2 \approx 213$$

and

$$E_{0,0} \approx -392 \text{ ev} \quad (6.17)$$

Thus, for  $N \sim 10^{12}$  gauss this model gives a ground state binding

energy of almost 400 ev. Figure 2 shows the variation of  $E_{a_0}$  with magnetic field strength, and Table 1 lists the energy levels for  $H \sim 10^{12}$  gauss. For such a magnetic field, there is a set of strongly bound states (binding energies in the range 200 to 400 ev), and a double set of states with binding energies in the usual hydrogen range 1 to 10 ev.

A difficulty here is the restriction inherent in the use of equations (6.12), namely

$$b_s \ll a_0 \quad (6.18)$$

i.e.

$$\sqrt{\frac{s+1}{Y}} \ll a_0 \quad (6.19)$$

This implies

$$H \geq 10^{11} \text{ gauss} \quad (6.20)$$

and for  $H \sim 10^{12}$  gauss

$$\sqrt{s+1} \ll 15 \quad (6.21)$$

Thus these results relate only to an electron that is close to the nucleus. The electron density of such a hydrogen atom is elongated along the magnetic field axis. The electron "shells" are now cylinders of length  $\sim a_0$ , radius  $\sim \sqrt{\frac{s+1}{Y}}$ , and thickness  $\sim \sqrt{\frac{1}{Y}}$ . One can immediately picture a multi-electron atom with the electrons stacked in the various cylindrical shells.

Considering further the levels enumerated in Table 1, transitions between such atomic levels would produce  $\sim 100$  ev photons (i.e.  $\lambda \sim 100 \text{ \AA}$ ). It remains to be seen in chapter 7 whether any unionized hydrogen can exist in the supposedly  $10^{12}$  gauss and  $10^6$  °K atmosphere of a neutron star. The high binding energy indicated here is only one new

aspect of three or four that enter into the computation of the ionization fraction.

Thus the one-dimensional truncated coulomb potential of Haines and Roberts gives a basic picture of the hydrogen atom in  $\sim 10^{12}$  gauss. It remains to improve the computation by using a proper coulomb potential and a suitable three-dimensional wave function (the radial function so far has been essentially a delta function, thereby constraining the electron to a magnetic field line).



### 6.3 Variational Calculation #1

A better estimate of the energy levels can be obtained by using  
(i) the one-dimensional coulomb potential

$$V(z) = \frac{-e^2}{\sqrt{b^2 + z^2}} \quad (6.22)$$

(ii) a suitable trial wave function, and (iii) variational calculus.

As a trial function, a suggested form is that of the ordinary hydrogen ground state wave function.

i.e.

$$f(z) = \left( \frac{A}{a_0} \right)^{1/2} e^{-\frac{A|z|}{a_0}} \quad (6.23)$$

A is then the variational parameter.

The results, of course, depend on 's'. Putting in the necessary subscripts gives

$$V_s(z) = \frac{-e^2}{\sqrt{b_s^2 + z^2}} \quad (6.24)$$

$$f_s(z) = \left( \frac{A_s}{a_0} \right)^{1/2} e^{-\frac{A_s|z|}{a_0}}$$

From equation (6.15)

$$b_s^2 \approx \langle r^2 \rangle_s = \frac{s+1}{Y} \quad (6.25)$$

The Schroedinger equation for the system is then

$$-\frac{\hbar^2}{2m} \frac{d^2 f_s(z)}{dz^2} - \frac{e^2}{\sqrt{b_s^2 + z^2}} f_s(z) = E_s f_s(z) \quad (6.26)$$

From variational calculus (Mathews and Walker 1965), the lowest eigenvalue is given by the absolute minimum of the functional

$$K[f_s(z)] = \frac{\hbar^2}{2m} \int_{-\infty}^{\infty} \frac{df_s(z)}{dz} dz - e^2 \int_{-\infty}^{\infty} \frac{[f_s(z)]^2}{\sqrt{b_s^2 + z^2}} dz \quad (6.27)$$

Substituting for  $f_s(z)$  gives

$$K[f_s(z)] = \frac{\hbar^2}{2m} \left( \frac{A_s}{a_0} \right)^2 - \frac{e^2 A_s}{a_0} \int_{-\infty}^{\infty} \frac{e^{-\frac{2A_s|z|}{a_0}}}{\sqrt{b_s^2 + z^2}} dz \quad (6.28)$$

The remaining integral can be evaluated using the relation  
(Gradshteyn and Ryzhik 1965)

$$\int_0^{\infty} (x^2 + a^2)^{(\nu-1)} e^{-\mu x} dx = \frac{\sqrt{\pi}}{2} \Gamma(\nu) \left( \frac{2a}{\mu} \right)^{\nu-1/2} \left[ H_{\nu-1/2}(u\mu) - N_{\nu-1/2}(u\mu) \right] \quad (6.29)$$

For  $\nu = \frac{1}{2}$  this reduces to

$$\int_0^{\infty} (x^2 + u^2)^{-1/2} e^{-\mu x} dx = \frac{\sqrt{\pi}}{2} \Gamma(1/2) [H_0(\mu u) - N_0(\mu u)] \quad (6.30)$$

Therefore

$$K[f_s(z)] = \frac{\hbar^2}{2m} \left( \frac{A_s}{a_0} \right)^2 - \pi e^2 \left( \frac{A_s}{a_0} \right) \left[ H_0\left(\frac{2A_s b_s}{a_0}\right) - N_0\left(\frac{2A_s b_s}{a_0}\right) \right] \quad (6.31)$$

Since  $A_s$  is expected to be on the order of 1, and keeping the condition  $b_s \ll a_0$ , the argument of the Bessel functions can be considered small. The approximations

$$H_0(2x) \sim \frac{x^{3/2}}{\Gamma(3/2)} \quad 2x \ll 1 \quad (6.32)$$

$$N_0(2x) \sim \frac{2}{\pi} \ln x \quad 2x \ll 1$$

can be used giving

$$K[f_s(z)] \approx \frac{\hbar^2}{2m} \left( \frac{A_s}{a_0} \right)^2 + 2e^2 \left( \frac{A_s}{a_0} \right) \ln \left( \frac{A_s b_s}{a_0} \right) \quad \frac{2A_s b_s}{a_0} \ll 1 \quad (6.33)$$

Since  $a_0 = \frac{\hbar^2}{me^2} \quad \frac{e^2}{2a_0} = 13.6 \text{ eV} \quad (6.34)$

$$K[f_s(z)] \approx 13.6 \left\{ A_s^2 + 4 A_s \ln \left( \frac{A_s b_s}{a_0} \right) \right\} \quad (6.35)$$

The condition for the absolute minimum of this functional is

$$\frac{\partial K[f_s(z)]}{\partial A_s} = 0 \quad (6.36)$$

$$\text{i.e.} \quad A_s + 2 \ln\left(\frac{A_s b_s}{a_0}\right) + 2 = 0 \quad (6.37)$$

Once this is solved numerically for  $A_s$ ,  $E_s$  is given by

$$E_s = -13.6 (A_s^2 + 4A_s) \quad (6.38)$$

The results are tabulated in Table 2 for  $H \sim 10^{12}$  gauss.

This set of states corresponds to the strongly bound set mentioned in section 6.2. These new energy values are somewhat lower than those suggested by the truncated coulomb potential. Now the hydrogen ground state binding energy in  $\sim 10^{12}$  gauss is estimated to be about 160 ev.

The other set of energy levels could be obtained by generating a set of even and odd trial functions and performing the variational calculation for each of them. This is what Camuto and Kelly did using perturbation theory and numerical methods. Their double set of binding energies is in the range 0 to 13.5 ev and the respective values are a bit higher than those in Table 1.

Thus the use of the truncated coulomb potential in section 6.2 introduced an error of about a factor of two. It is now necessary to see to what extent the variational calculation can be improved. A better trial wave function should give a lower energy value  $E_s$  (i.e. a higher binding energy). This is indeed found to be the case in the

next section.

## 6.4 Variational Calculation #2

A somewhat cumbersome improvement to the previous calculation is the use of a three-dimensional coulomb potential and wave function. The coulomb potential is

$$V(r, z) = \frac{-e^2}{\sqrt{r^2 + z^2}} \quad (6.39)$$

For a trial wave function, a possibility is a combination of a gaussian in the z-coordinate and the radial part of the wave function of a free electron in a magnetic field.

i.e.

$$\Psi_s(r, z) = \sqrt{2\gamma} \left( \frac{e^{-r} r^s}{s!} \right)^{1/2} \left( \frac{\alpha_s}{\sqrt{\pi}} \right)^{1/2} e^{-\frac{\alpha_s^2 z^2}{2}} \quad (6.40)$$

$$e = \gamma r^2$$

$\alpha_s$  is now the variational parameter.  $V_s(z)$  can be defined as

$$V_s(z) = -e^2 \int_0^\infty \frac{e^{-r} r^s}{s!} \frac{1}{\sqrt{\gamma^{-1} r^2 + z^2}} dr \quad (6.41)$$

Using the relations

$$\int_0^\infty \frac{e^{-\mu x} dx}{\sqrt{x+\beta}} = \sqrt{\frac{\pi}{\mu}} e^{\beta\mu} \left[ 1 - \Phi(\sqrt{\beta\mu}) \right] \quad (6.42)$$

and

$$\Phi(x) = 1 - \frac{e^{-x^2/2}}{\sqrt{\pi x}} W_{-1/4, 1/4}(x^2) \quad (6.43)$$

and considering only the  $s=0$  case, gives

$$V_0(z) = -e^2 \sqrt{\gamma} \frac{e^{-\gamma z^2}}{\sqrt{\gamma^{1/2} |z|}} W_{-1/4, 1/4}(\gamma z^2) \quad (6.44)$$

The expectation value of this potential is needed in order to get the functional  $K[f_0(z)]$  as in equation (6.27). Here

$$f_0(z) = \left( \frac{\alpha_0}{\sqrt{\pi}} \right)^{1/2} e^{-\frac{\alpha_0^2 z^2}{2}} \quad (6.45)$$

Therefore

$$\begin{aligned} \langle V_0(z) \rangle &= \int_{-\infty}^{\infty} f_0(z) V_0(z) dz \\ &= -2e^2 \sqrt{\gamma} \int_0^{\infty} \frac{e^{-\gamma z^2}}{\sqrt{\gamma^{1/2} z}} W_{-1/4, 1/4}(\gamma z^2) \frac{\alpha_0}{\sqrt{\pi}} e^{-\frac{\alpha_0^2 z^2}{2}} dz \end{aligned} \quad (6.46)$$

$$\text{Let } \beta = \gamma z^2$$

$$(6.47)$$

Then

$$\langle V_0(z) \rangle = -\frac{e^2 \alpha_0}{\sqrt{\pi}} \int_0^{\infty} e^{-(\frac{\alpha_0^2}{\gamma} - \frac{1}{2})\beta} W_{-1/4, 1/4}(\beta) \frac{d\beta}{\beta} \quad (6.48)$$

Using the integral relation (Gradshteyn and Ryzhik 1965)

$$\int_0^{\infty} e^{-sx} W_{\kappa, \mu}(x) \frac{dx}{x} = \frac{\pi}{\cos \frac{\pi \mu}{2}} \left( \frac{s - \frac{1}{2}}{s + \frac{1}{2}} \right)^{\kappa/2} P_{\mu - \frac{1}{2}}^{\kappa}(2s) \quad (6.49)$$

$$\operatorname{Re}(\frac{1}{2} \pm \mu) > 0 \quad \operatorname{Re} s > -\frac{1}{2}$$

and the relation

$$P_{\nu}^{\mu}(z) = \left( \frac{z+1}{z-1} \right)^{\mu/2} \frac{1}{\Gamma(1-\mu)} F(-\nu, \nu+1, 1-\mu; \frac{1-z}{2}) \quad (6.50)$$

gives

$$\langle V_0(z) \rangle = -\frac{e^2 \alpha_0 \sqrt{\pi}}{\cos \pi/8} \frac{1}{\Gamma(5/4)} F(1/4, 3/4, 5/4; 1 - \alpha^2/8) \quad (6.51)$$

The argument of the above hypergeometric function can be changed using the transformation (Mathews and Walker 1965)

$$\begin{aligned} F(a, b, c; z) &= \frac{\Gamma(c) \Gamma(c-a-b)}{\Gamma(c-a) \Gamma(c-b)} F(a, b, 1+a+b-c; 1-z) \\ &+ \frac{\Gamma(c) \Gamma(a+b-c)}{\Gamma(a) \Gamma(b)} (1-z)^{c-a-b} F(c-a, c-b, 1+c-a-b, 1-z) \end{aligned} \quad (6.52)$$



i.e.

$$\langle V_0(z) \rangle = \frac{-e^2 \alpha_0 \sqrt{\pi}}{\cos \pi/8} \left\{ \frac{\Gamma(1/4)}{\Gamma(1) \Gamma(1/2)} F\left(\frac{1}{4}, \frac{3}{4}, \frac{3}{4}; \frac{\alpha_0^2}{8}\right) + \frac{\Gamma(-1/4)}{\Gamma(1/4) \Gamma(3/4)} \left(\frac{\alpha_0^2}{8}\right)^{1/4} F\left(1, \frac{1}{2}, \frac{5}{4}; \frac{\alpha_0^2}{8}\right) \right\} \quad (6.53)$$

The usefulness of this form lies in the expectation that  $\frac{\alpha_0^2}{8}$  is very small. From the form of  $f_0(z)$ ,  $\alpha_0$  is expected to be on the order of  $1/a_0$ .

Then

$$\frac{\alpha_0^2}{8} \sim \frac{1}{a_0^2} \ll 1 \quad (6.54)$$

for  $\hbar \sim 10^{12}$  gauss.

The hypergeometric function can now be expanded to lowest order in  $\frac{\alpha_0^2}{8}$ .

$$F\left(\frac{1}{4}, \frac{3}{4}, \frac{3}{4}; \frac{\alpha_0^2}{8}\right) \approx 1 + \frac{1}{4} \frac{\alpha_0^2}{8} \quad (6.55)$$

$$F\left(1, \frac{1}{2}, \frac{5}{4}; \frac{\alpha_0^2}{8}\right) = 1 + \frac{2}{5} \frac{\alpha_0^2}{8}$$

Then

$$\langle V_0(z) \rangle \approx \frac{-e^2 \alpha_0 \sqrt{\pi}}{\cos \pi/8} \left\{ \frac{\Gamma(1/4)}{\sqrt{\pi}} - \frac{4}{\Gamma(1/4)} \left(\frac{\alpha_0^2}{8}\right)^{1/4} \right\} \quad (6.56)$$

Since

$$\Gamma(1/4) = 3.63$$

$$\cos \pi/8 = .924$$

$$\langle V_0(z) \rangle \approx -1.92 e^2 \alpha_0 \{ 2.05 - 1.10 \left(\frac{\alpha_0^2}{8}\right)^{1/4} \} \quad (6.57)$$

The required functional  $K[f_0(z)]$  is therefore

$$K[f_0(z)] \approx \frac{\hbar^2 \alpha_0^2}{4m} - e^2 \alpha_0 \left\{ 3.93 - 2.12 \left( \frac{\alpha_0^2}{\gamma} \right)^{1/4} \right\} \quad (6.58)$$

Applying the stationary value condition  $\frac{\partial K}{\partial \alpha_0} = 0$  gives

$$\frac{\hbar^2 \alpha_0^2}{2m} - 3.93 e^2 + 3.18 e^2 \gamma^{-1/4} \alpha_0^{1/2} = 0 \quad (6.59)$$

$$\text{i.e.} \quad \alpha_0 - 7.86 \alpha_0^{-1} + 6.36 \alpha_0^{-1} \gamma^{-1/4} \alpha_0^{1/2} = 0 \quad (6.60)$$

Let  $\chi^2 = \alpha_0 a_0$

$$\text{Then} \quad \chi^2 + 6.36 (\gamma a_0^2)^{-1/4} \chi - 7.86 = 0 \quad (6.61)$$

$$\text{For } H \sim 10^{12} \text{ gauss} \quad \gamma a_0^2 \approx 213$$

Thus

$$\chi^2 + 1.67 \chi - 7.86 = 0 \quad (6.62)$$

The solution of this quadratic is  $\chi = 2.09$ . Therefore

$$\alpha_0 = \frac{4.36}{a_0} \quad (6.63)$$

Substituting this result in equation (6.58) gives

$$E_0 \approx -14.6 \left( \frac{e^2}{2a_0} \right) = -198 \text{ ev} \quad (6.64)$$

Thus this somewhat more accurate variational calculation gives a ground state binding energy of about 200 ev for hydrogen in a magnetic field of  $\sim 10^{12}$  gauss. This is 20% higher than the 160 ev computed in the earlier variational calculation and reflects the better trial wave function. The other strongly bound levels could be computed as well

but the computation is rather lengthy. Suffice it to say that the ground state binding energy is  $\sim 200$  ev and the other levels are about those given in Table 2 multiplied by 1.2 .

The wave function (6.40) clearly demonstrates the cylindrical shell picture. The radial probability density has the form  $e^{-e} e^s$  giving a root mean square radius of  $\sqrt{\frac{s+1}{s}}$  . The shells overlap to a certain extent as shown in Fig. 3 .

Finally, the gaussian envelope  $e^{-\alpha_s^2 z^2}$  pinches off the cylindrical shells. For  $s=0$ ,  $\alpha_0 = \frac{4.36}{a_0}$  implies a half-width of  $\sim \frac{a_0}{2}$  for the electron probability density along the magnetic field direction. In other words, the scale length for the electron motion along  $\vec{H}$  is, not surprisingly, the regular Bohr radius ( $\sim 5 \times 10^{-9}$  cm). Since the radial scale length is  $\sqrt{\frac{r}{s}} (\sim 3 \times 10^{-10}$  cm. for  $H \sim 10^{12}$  gauss), the  $s=0$  cylindrical shell is highly eccentric with a length-radius ratio of  $\sim 17$  . Thus the ground state hydrogen atom in  $\sim 10^{12}$  gauss looks very much like a cigar.

## Chapter 7

### IONIZATION FRACTION

#### 7.1 Statistics

It has been established in chapter 6 that the hydrogen ground state binding energy in  $\sim 10^{12}$  gauss is about 200 ev. The question then arises as to what effect this will have on the ionization fraction of a hydrogen plasma in such an environment. Parallel with this consideration is the question of what statistics are appropriate for such conditions (e.g.  $B \sim 10^{12}$  gauss,  $\rho \sim 1$  gm/cm<sup>3</sup>,  $T \sim 10^6$  °K; "typical" surface conditions of neutron star models; Chiu and Canuto 1969).

The energy spacing between the various magnetic quantum levels of a free electron in a homogeneous magnetic field of  $\sim 10^{12}$  gauss is about  $10^4$  ev. For  $kT \ll 10^4$  ev essentially all free electrons will be in the ground state assuming a purely Boltzmann factor is applicable. In particular, for  $T \sim 10^6$  K,  $kT \sim 86$  ev  $\ll 10^4$  ev.

The Boltzmann approximation is valid if the occupation number  $n(\epsilon)$  is much less than the statistical weight  $g(\epsilon)$  (Crawford 1963). For an electron in a magnetic field

$$g(\epsilon) = \frac{V \gamma}{\pi h} \sqrt{\frac{m}{2\epsilon}} \quad (7.1)$$

where  $V$  is the volume and  $\epsilon$  is the electron kinetic energy. This

result is derived from the magnetic statistical weight  $\frac{\gamma}{\pi}$  (Canuto and Chiu 1968), and the one-dimensional phase space factor

$$\frac{dp}{h} = \sqrt{\frac{m}{2\epsilon}} \frac{d\epsilon}{h} \quad (7.2)$$

Assuming a Boltzmann distribution, i.e.

$$n(\epsilon) = g(\epsilon) e^{-\alpha - \beta\epsilon} \quad \alpha + \beta\epsilon \gg 1 \quad (7.3)$$

the total number N of electrons and their total energy E are given by

$$N = \int_0^{\infty} n(\epsilon) d\epsilon = \int_0^{\infty} g(\epsilon) e^{-\alpha - \beta\epsilon} d\epsilon = \frac{V\gamma}{\pi h} \sqrt{\frac{m}{2}} e^{-\alpha} \int_0^{\infty} \frac{e^{-\beta\epsilon}}{\sqrt{\epsilon}} d\epsilon$$

$$E = \int_0^{\infty} \epsilon n(\epsilon) d\epsilon = \int_0^{\infty} \epsilon g(\epsilon) e^{-\alpha - \beta\epsilon} d\epsilon = \frac{V\gamma}{\pi h} \sqrt{\frac{m}{2}} e^{-\alpha} \int_0^{\infty} e^{-\beta\epsilon} \sqrt{\epsilon} d\epsilon$$

i.e.

$$N = \frac{V\gamma}{\pi h} \sqrt{\frac{m}{2}} e^{-\alpha} \sqrt{\frac{\pi}{\beta}} \quad (7.4)$$

$$E = \frac{V\gamma}{\pi h} \sqrt{\frac{m}{2}} e^{-\alpha} \frac{\sqrt{\pi}}{2\beta\sqrt{\beta}}$$

Then

$$\beta = \frac{N}{2E} = \frac{1}{2\bar{\epsilon}} \quad (7.5)$$

Since  $\bar{\epsilon} = \frac{1}{2}kT$  for one-dimensional motion

$$\beta = \frac{1}{kT} \quad (7.6)$$

as is the case in classical statistical mechanics.

Solving now for  $e^{-\alpha}$ ,

$$e^{-\alpha} = N \frac{\pi h}{V \delta} \sqrt{\frac{2}{m}} \sqrt{\frac{\beta}{\pi}} = \frac{N}{V} \frac{2\pi}{\delta} \left( \frac{h^2}{2\pi m k T} \right)^{1/2} \quad (7.7)$$

Therefore

$$\alpha = \ln \left\{ \frac{V}{N} \frac{\delta}{2\pi} \sqrt{\frac{2\pi m k T}{h^2}} \right\} \quad (7.8)$$

which is quite similar to the usual three-dimensional form

$$\alpha^{3-D} = \ln \left\{ \frac{V}{N} \left( \frac{2\pi m k T}{h^2} \right)^{3/2} \right\} \quad (7.9)$$

The classical approximation condition is simply

$$e^{-\alpha} \ll 1 \quad (7.10)$$

since

$$e^{-\beta \epsilon} \approx e^{-\beta \bar{\epsilon}} = e^{-1/2} = .6 \quad (7.11)$$

i.e.

$$\frac{N}{V} \frac{2\pi}{\delta} \left( \frac{h^2}{2\pi m k T} \right)^{1/2} \ll 1 \quad (7.12)$$

This reduces to

$$\frac{N}{V} \ll 1.6 \times 10^{11} \text{ } \delta \sqrt{T} \quad (7.13)$$

For  $\mathcal{H} \sim 10^{12}$  gauss and  $T \sim 10^6$  K this means

$$\frac{N}{V} \ll 1.6 \times 10^{26} \quad (7.14)$$

For a matter density of  $\sim 1$  gm/cm<sup>3</sup>, and assuming charge neutrality,

$$\frac{N}{V} \leq 10^{24} \quad (7.15)$$

which certainly satisfies the above condition.

Another way to show the validity of the classical approximation for these conditions is by calculating the Fermi energy and showing that it is much less than  $kT$ . The total number of electrons at  $0^\circ\text{K}$  is given by

$$\begin{aligned} N &= \int_0^{\epsilon_F^0} g(\epsilon) d\epsilon \\ &= \int_0^{\epsilon_F^0} \frac{V\gamma}{\pi h} \sqrt{\frac{\pi}{2}} \frac{d\epsilon}{\sqrt{\epsilon}} \\ &= \frac{V\gamma}{\pi h} \sqrt{2m} (\epsilon_F^0)^{1/2} \end{aligned} \quad (7.16)$$

i.e. 
$$\epsilon_F^0 = \frac{\pi^2 h^2}{2m\gamma^2} \left( \frac{N}{V} \right)^2 \quad (7.17)$$

For  $\frac{N}{V} \approx 10^{24}$  and  $\mathcal{H} \sim 10^{12}$  gauss, this Fermi energy is  $\sim 10^{-3}$  ev which is certainly much less than  $kT$  for  $T \sim 10^6$  K.

This classical approximation is helped by the magnetic phase factor

$\frac{\gamma}{\pi}$  being somewhat larger than the  $\frac{4\pi p^2}{h^2}$  factor used in "ordinary" situations.

For  $H \sim 10^{12}$  gauss

$$\frac{\gamma}{\pi} \approx 2 \times 10^{18}$$

(7.18)

For  $T \sim 10^6$  K

$$\frac{4\pi p^2}{h^2} \approx \frac{4\pi mkT}{h^2} \approx 5 \times 10^{16}$$

The higher statistical weight means a lower Fermi energy and a "more" classical statistical at high temperatures.



## 7.2 Ionization Fraction

The ionization fraction is obtained by slightly modifying the Saha equation. If  $dN_e$  is the number of free electrons with z-momenta in the interval  $(p_z, p_z + dp_z)$ , and  $N_H^0$  is the number of unionized ground state hydrogen atoms, Boltzmann statistics gives

$$\frac{dN_e}{N_H^0} = \frac{g_e}{g_H^0} e^{-\frac{p_z^2}{2mkT} - \frac{\phi}{kT}} dp_z \quad (7.19)$$

where  $\phi$  is the ionization potential.

From equation (7.1)

$$g_e = \frac{V\lambda}{\pi h}$$

Therefore

$$\frac{N_e}{N_H^0} = \frac{1}{g_H^0} \frac{V\lambda}{\pi h} (2\pi mkT)^{1/2} e^{-\phi/kT} \quad (7.20)$$

Of course there will be hydrogen atoms in states other than the ground state. The total number  $N_H$  of unionized hydrogen atoms is

$$N_H = \sum_j N_H^j = \sum_j N_H^0 \frac{g_H^j}{g_H^0} e^{-\frac{(E_j - E_0)}{kT}} = \frac{N_H^0}{g_H^0} Q(T) \quad (7.21)$$

where  $Q(T)$  is the partition function.

i.e.

$$Q(\tau) = \sum_j g_H^j e^{-\frac{(E_j - E_0)}{kT}} \quad (7.22)$$

Therefore

$$\frac{N_e}{N_H} = \frac{1}{Q(\tau)} \frac{V \gamma}{\pi h} (2\pi m k T)^{1/2} e^{-\phi/kT} \quad (7.23)$$

This is the modified Saha equation referred to earlier.  $V$  can be chosen such that it contains one ionized atom. Then

$$N_{H^+} V = 1 \quad (7.24)$$

where  $N_{H^+}$  is the number density of ionized atoms.  $N_e$  and  $N_H$  can also be treated as number densities since they occur in a ratio. Therefore

$$\frac{N_e N_{H^+}}{N_H} = \frac{1}{Q(\tau)} \frac{\gamma}{\pi h} (2\pi m k T)^{1/2} e^{-\phi/kT} \quad (7.25)$$

The ionization fraction  $f$  is given by

$$f = \frac{N_{H^+}}{N_H + N_{H^+}} \quad (7.26)$$

The matter density  $\rho$  is

$$\rho = (N_H + N_{H^+}) M_H \quad (7.27)$$

Then 
$$f = \frac{N_{H^+} M_H}{\rho} \quad \text{i.e.} \quad N_{H^+} = \frac{\rho f}{M_H} \quad (7.28)$$

Moreover 
$$\frac{N_{H^+}}{N_H} = \frac{f}{1-f} \quad (7.29)$$

Assuming charge neutrality, i.e.  $N_e = N_{H^+}$

$$\frac{N_e N_{H^+}}{N_H} = \frac{(N_{H^+})^2}{N_H} = \frac{\rho}{M_H} \frac{f^2}{1-f} \quad (7.30)$$

Finally

$$\frac{f^2}{1-f} = \frac{M_H}{\rho} \frac{1}{Q(T)} \frac{8}{\pi} \left( \frac{2\pi m k T}{h^2} \right)^{1/2} e^{-\phi/kT} \quad (7.31)$$

For  $T \sim 10^6$  °K,  $\rho \sim 1$  gm/cm<sup>3</sup>, and  $\phi \sim 200$  ev,

$$\frac{f^2}{1-f} \approx \frac{45}{Q(10^6)} \quad (7.32)$$

There remains the problem of estimating the partition function  $Q(10^6)$ . This is difficult enough in ordinary cases due to the broadening of the energy levels by various perturbations (Motz 1970). Some sort of form factor often has to be introduced.

A primary consideration is the depression  $\Delta E$  of the continuum due to electrostatic effects. A simple estimate of  $\Delta E$  is (Cox and Giuli 1968)

$$\Delta E \approx \frac{e^2}{2r_0} \quad (7.33)$$

where  $r_0$  is the average interatomic distance.

i.e. 
$$n_0 = .735 \times 10^{-8} \rho^{-1/3} \text{ cm.} \quad (7.34)$$

with  $\rho$  in  $\text{gm/cm}^3$ .

For  $\rho \sim 1 \text{ gm/cm}^3$  this means

$$n_0 = .735 \times 10^{-8} \text{ cm.} \quad (7.35)$$

and 
$$\Delta E \approx 11 \text{ ev.} \quad (7.36)$$

Thus the continuum is depressed by about 11 ev. This means that essentially all the double set of levels in the 0 to 10 ev range are smeared into the continuum. Furthermore the ionization potential is ~11 ev less than the 200 ev computed in section 6.4 .

Therefore the partition function  $Q(T)$  need only include the tightly bound set of states. There are about five of these for  $H \sim 10^{12}$  gauss, since according to (6.21)

$$\sqrt{s+1} \ll 15 \quad (7.37)$$

i.e. 
$$s \leq 4 \quad (7.38)$$

Using 1.2 times the values in Table 1 and assuming unit statistical weight

$$Q(T) = 1 + \exp\left(-\frac{3E_H}{kT}\right) + \exp\left(-\frac{4.6E_H}{kT}\right) + \exp\left(-\frac{5.5E_H}{kT}\right) + \exp\left(-\frac{6.2E_H}{kT}\right) \quad (7.39)$$

For  $T \sim 10^6 \text{ K}$ ,  $kT \approx 86 \text{ ev}$

i.e. 
$$Q(10^6) \approx 3 \quad (7.40)$$

Then in (7.32)

$$\frac{f^2}{1-f} \approx 15$$

(7.41)

$$\text{i.e. } f \approx .93$$

The estimated ionization fraction is ~93%. Thus the high binding energy does succeed in keeping some of the hydrogen atoms in the ground state despite a temperature of  $\sim 10^6$  K, a larger phase space (a factor of 40 according to (7.18)), and an 11 eV depression of the continuum.

Therefore the atmosphere is highly ionized, but thanks to the magnetic field of  $\sim 10^{12}$  gauss some unionized hydrogen can exist, and its level transitions will add to the  $\sim 100$  Å emission of the star.

## Chapter 8

### A "THOMAS-FERMI MODEL"

It is possible to extend the considerations of chapters 6 and 7 to larger atoms by Hartree calculations (Cohen et al. 1970) and by modifying the Thomas-Fermi atomic model. It is the latter approach that will be used in this chapter.

As has been shown previously, the usual electron phase space factor  $2 \cdot \frac{4\pi p^2 dp}{h^3}$  must be replaced by  $\frac{\gamma}{\pi} \frac{dp}{h}$ . The electron density per unit momentum interval is then

$$d^2 n = \frac{\gamma}{\pi} \frac{dp}{h} d\tau = \frac{\gamma}{\pi} \frac{dp}{h} 4\pi r^2 dr \quad (8.1)$$

where  $r$  is now a spherical coordinate. The derivation then proceeds as in the usual case (Leighton 1959).

$$dn = \frac{\gamma}{\pi} p_0 \frac{4\pi r^2 dr}{h} \quad (8.2)$$

$$\text{where} \quad p_0 = (-2mV)^{1/2} \quad (8.3)$$

and  $V(r)$  is the electron potential.

Gauss' Law gives

$$-r^2 \frac{dV}{dr} = -Ze^2 + e^2 \int_0^r \frac{dn}{dr} dr \quad (8.4)$$

Differentiating this equation yields

$$-\frac{d}{d\lambda} \left( \lambda^2 \frac{dV}{d\lambda} \right) = e^2 \frac{dn}{d\lambda} = e^2 \frac{\gamma}{\pi} \left( \frac{-2mV}{h} \right)^{1/2} 4\pi\lambda^2 \quad (8.5)$$

Let

$$V(\lambda) = -\frac{Ze^2}{\lambda} \chi \quad (8.6)$$

and

$$\lambda = \alpha x$$

define the dimensionless variables  $\chi$  and  $x$ . Then

$$\frac{1}{\alpha^2} \frac{d^2\chi}{dx^2} = \frac{1}{Z} \frac{\gamma}{h} (2mZe^2)^{1/2} 4 \chi^{1/2} \alpha^{1/2} x^{1/2} \quad (8.7)$$

i.e.

$$\frac{d^2\chi}{dx^2} = \chi^{1/2} x^{1/2} \quad (8.8)$$

with

$$\alpha = \left\{ \frac{Zh}{4\gamma} (2mZe^2)^{-1/2} \right\}^{2/5} \quad (8.9)$$

This compares with  $\chi'' = \chi^{3/2} x^{-1/2}$  for the ordinary case. The boundary conditions on  $\chi$  are the same, namely

$$\begin{aligned} \chi(0) &= 1 \\ \chi(\infty) &= 0 \end{aligned} \quad (8.10)$$

Equation (8.8) has been solved numerically (Kadomstev 1970).

The expression for  $\alpha$  gives an estimate of the atomic size. The atomic radius is

$$R \approx \alpha = \left\{ \frac{h}{4} (2me^2)^{-1/2} \right\}^{2/5} \frac{Z^{1/5}}{H^{2/5}} \quad (8.11)$$

Since  $\gamma = \frac{eH}{2\hbar c}$

$$R \approx \left\{ \frac{h^2 c}{4\pi e} (2me^2)^{-1/2} \right\}^{2/5} \frac{Z^{1/5}}{H^{2/5}} = 37 \times 10^{-6} \frac{Z^{1/5}}{H^{2/5}} \text{ cm.} \quad (8.12)$$

For  $H \sim 10^{12}$  gauss

$$R \approx 6 \times 10^{-10} Z^{1/5} \text{ cm.} \quad (8.13)$$

Thus a larger magnetic field results in a smaller atom. This is expected since a larger magnetic field means closer "orbits". Of course the use of spherical symmetry here is valid only if the number of electrons is sufficiently large that the elongation of the electron density, mentioned previously in regard to the hydrogen atom, is blurred out by electron "far" from the nucleus.

i.e.

$$\sqrt{\frac{s_{\max} + 1}{\gamma}} \geq \frac{a_0}{Z} \quad (8.14)$$

$$\text{i.e.} \quad Z^3 \geq a_0^2 \gamma \quad (8.15)$$



Putting  $s_{\max} \sim Z$  is assuming one electron per shell on the average. In terms of the magnetic field  $\mathcal{H}$  the condition is

$$Z^3 \geq 2 \times 10^{-10} \mathcal{H} \quad (8.16)$$

For  $\mathcal{H} \sim 10^{12}$  gauss this means

$$Z^3 \geq 200 \quad (8.17)$$

i.e.

$$Z \geq 6 \quad (8.18)$$

Therefore, for  $\mathcal{H} \sim 10^{12}$  gauss the Thomas-Fermi approach is applicable to atoms with  $Z \geq 6$ . The "atomic radius" is given by (8.13), and the atom can be pictured as a series of cylindrical shells with the radius of the outer shell of the same order of magnitude as its length. The spherical nature of the atom is also enhanced by the large overlap of the outer shells.

$$\Psi_s^2(\rho) \sim e^{-\rho} \rho^s \quad (8.19)$$

$$\frac{\Psi_s^2(s+1)}{\Psi_s^2(s)} \approx e^{-1} \left( \frac{s+1}{s} \right)^s \approx 1 \quad \text{large } s \quad (8.20)$$

i.e. the space probability density  $\Psi_s^2(\rho)$  has a very broad peak at  $\rho = s$  for large 's'.

Finally, the electron density is given by

$$\frac{dn}{d\tau} = \frac{\gamma}{\pi} \frac{P_0}{h} \quad (8.22)$$

$$= \frac{\gamma}{\pi} \left( \frac{-2mV}{h} \right)^{1/2} \quad (8.23)$$

$$= \frac{\gamma}{\pi h} \left( \frac{2mZe^2}{a} \right)^{1/2} \frac{\chi}{x^{1/2}} \quad (8.24)$$

Given the numerical solution to (8.8), this electron density could be plotted explicitly for particular  $Z, \mu$  combinations.

# Chapter 9

## CONCLUSIONS AND DISCUSSION

For hydrogen atoms in intense magnetic fields:

- (1) The "Bohr" picture does not allow bound states for  $H \geq 4 \times 10^9$  gauss.
- (2) The truncated coulomb potential

$$V_s = \frac{-e^2}{|z| + b_s} \quad (9.1)$$

with

$$b_s = \sqrt{\frac{s+1}{8}}$$

gives a set of strongly bound states ( $E_0 = -392$  ev,  $E_1 = -299$  ev, etc. for  $H \sim 10^{12}$  gauss) and a double set of "hydrogen-like" states ( $E = -10$  ev).

- (3) A variational calculation using

$$V_s = \frac{-e^2}{\sqrt{b_s^2 + z^2}} \quad (9.2)$$

$$f_s(z) = \left(\frac{A_s}{a_0}\right)^{1/2} e^{-\frac{A_s |z|}{a_0}}$$

gives lower binding energies for the strongly bound states ( $E_0 = -160$  ev,  $E_1 = -128$  ev, etc.).

- (4) A further variational calculation using

$$V = \frac{-e^2}{\sqrt{r^2 + z^2}} \quad (9.3)$$

$$\psi_s(\rho, z) = \sqrt{2\gamma} \left( \frac{e^{-\rho} \rho^s}{s!} \right)^{1/2} \left( \frac{\alpha_s}{\sqrt{\pi}} \right)^{1/2} e^{-\frac{\alpha_s^2 z^2}{2}}$$

gives a binding energy of  $\sim 200$  ev for the hydrogen ground state when  $H \sim 10^{12}$  gauss.

These results are consistent with those obtained by other workers. Cohen et al. (1970) got a hydrogen ground state of  $\sim -160$  ev for  $H = 2 \times 10^{12}$  gauss using a Hartree calculation. They also extended their calculation to multi-electron atoms of low Z. Camuto and Kelly got  $E_0 \approx -190$  ev for  $H \approx 2 \times 10^{12}$  gauss by numerical methods similar to (4), and with perturbation methods also obtained the double set of hydrogen-like states.

The "Saha" equation for thermal ionization in an intense magnetic field is

$$\frac{N_e N_{H^+}}{N_H} = \frac{\delta}{\pi h} \frac{(2\pi m k T)^{1/2}}{Q(T)} e^{-\phi/kT} \quad (9.4)$$

provided  $kT \ll \hbar \omega_c$

and  $N/V \ll 1.6 \times 10^{22} H \sqrt{T}$

For a "typical" neutron star atmosphere ( $\rho \sim 1$  gm/cm<sup>3</sup>,  $T \sim 10^6$  K),  $\phi \sim 200$  ev implies an ionization fraction of perhaps 90%. The larger free electron phase space compensates for the higher ionization potential.

A modified Thomas-Fermi model indicates smaller atomic size for

stronger magnetic fields. The atomic dimension is given by

$$R \approx 37 \times 10^{-6} Z^{1/5} \hbar^{-2/5} \text{ cm.} \quad (9.5)$$

and the differential equation form is now

$$\chi'' = \chi^{1/2} x^{1/2} \quad \begin{array}{l} \chi(0) = 1 \\ \chi(\infty) = 0 \end{array} \quad (9.6)$$

as compared with the non-magnetic version.

$$\chi'' = \chi^{3/2} x^{-1/2} \quad (9.7)$$

Kadomstev (1970) also derived (9.6) and besides solving it numerically, he studied its regions of applicability in some detail.

Therefore, the overall picture of atomic structure in an intense magnetic field is one of electrons moving in cylindrical shells (length  $\sim a_0$ , radius  $\sim \sqrt{\frac{5+1}{8}}$ , thickness  $\sqrt{\frac{1}{8}}$ ). For hydrogen the elongation in the electron density is quite pronounced, but for high  $Z$  a degree of spherical symmetry returns.

Figure 1: The "Bohr" Picture

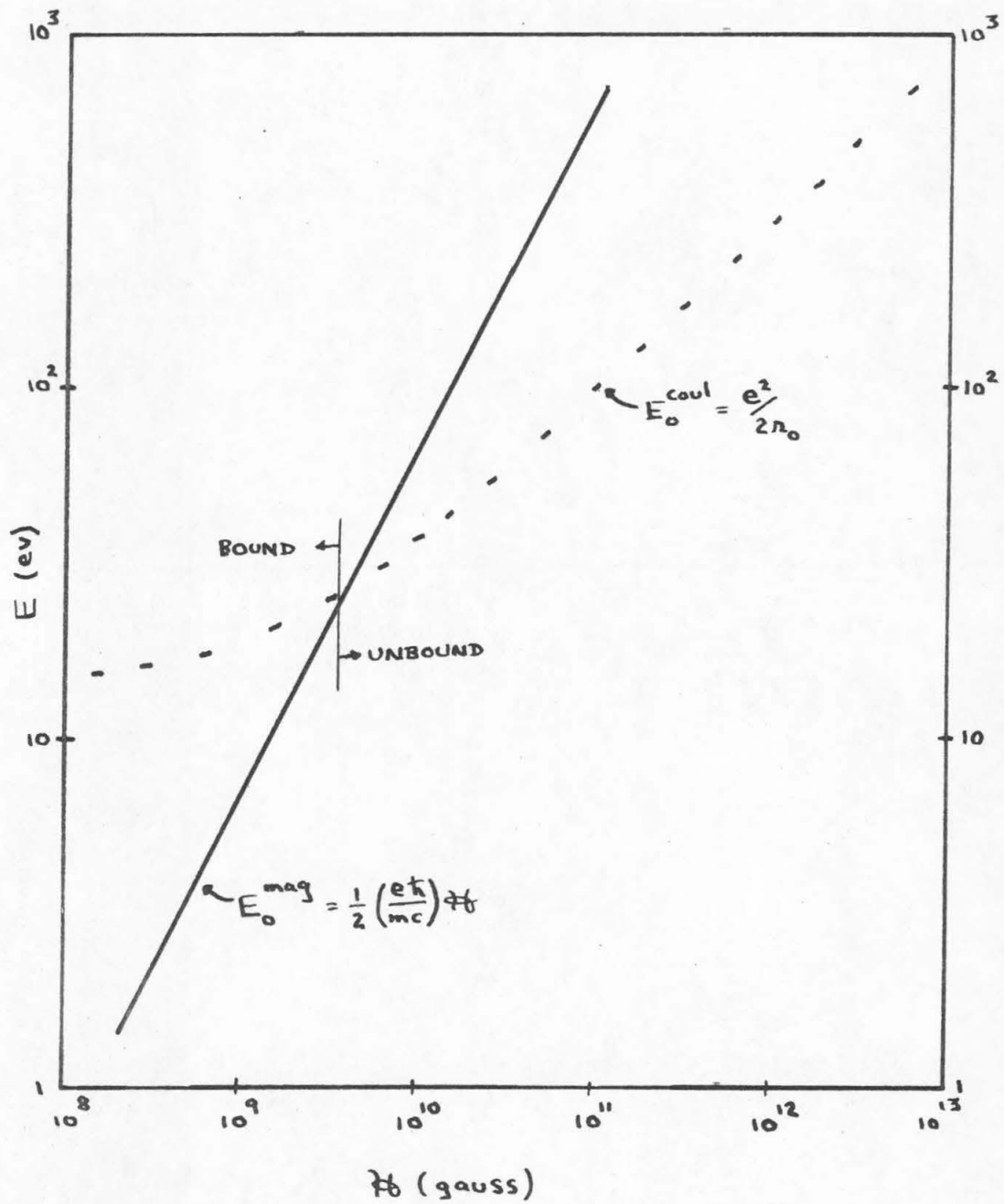


Figure 2: Hydrogen Ground State Energy  $E_{0,0} = -\frac{\hbar^2}{2ma_0^2} [\ln(\gamma a_0^2)]^2$

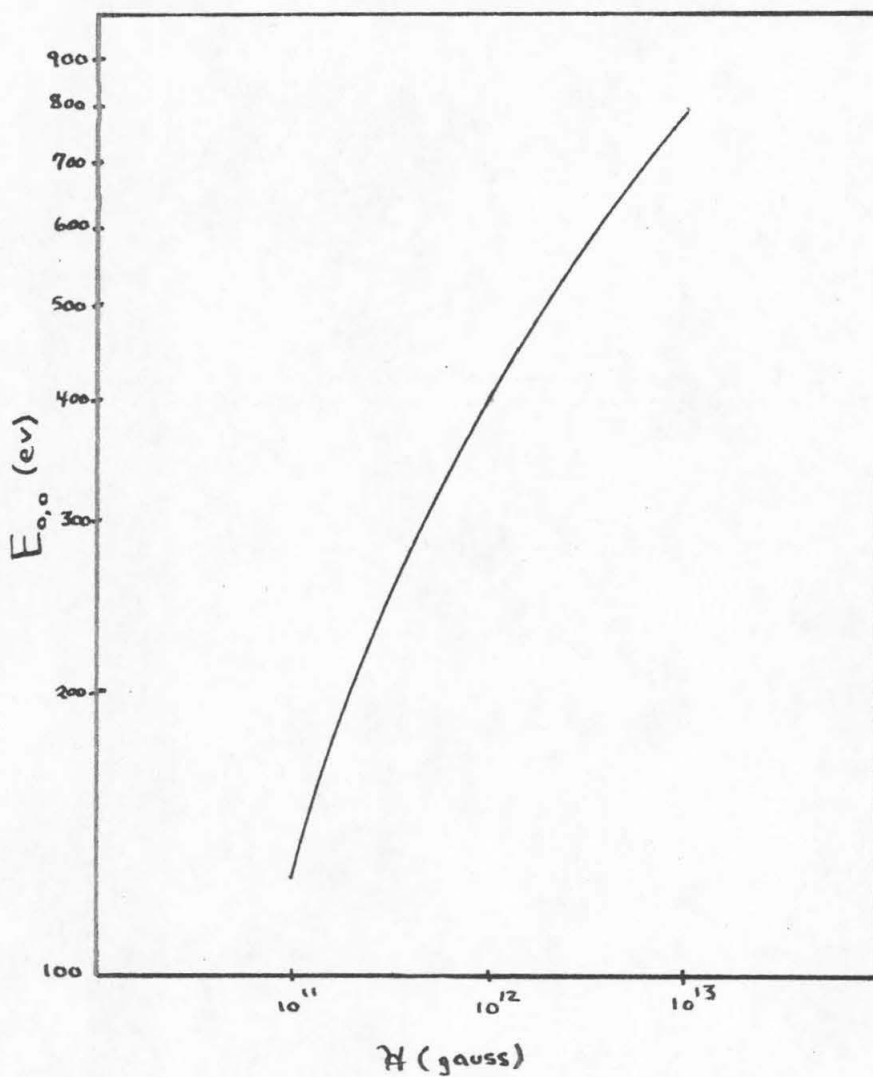


Figure 3: "Cylindrical Shells".

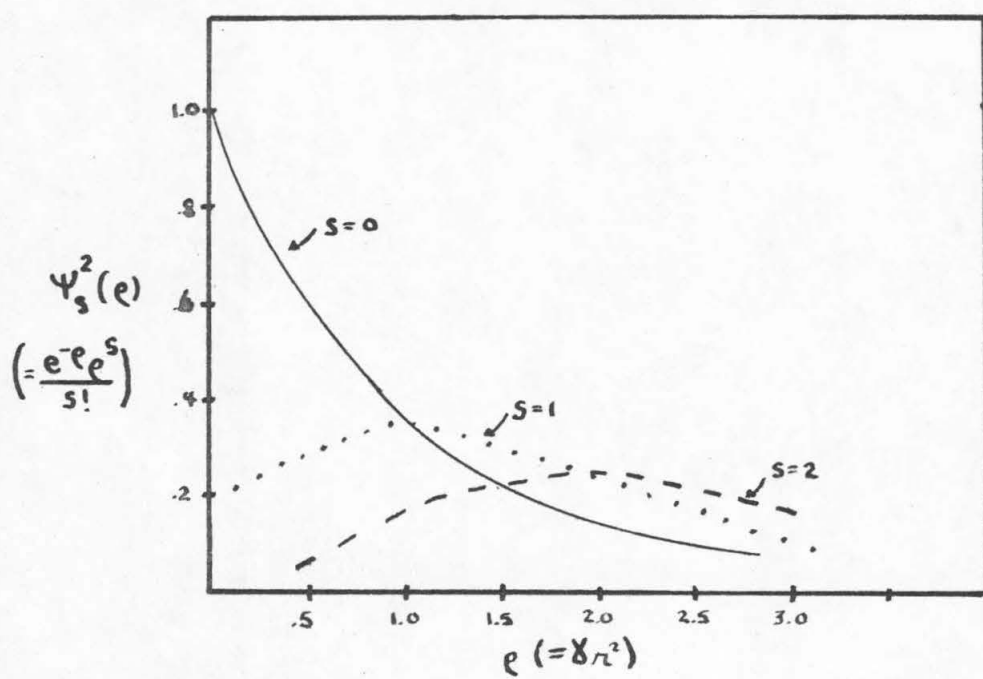




Table 1 : Hydrogen binding energies (in units of  $E_H = -13.6$  ev) computed with the truncated coulomb potential for  $H = 10^{12}$  gauss.

s	$E_{0,s}/E_H$	$E_{1,s}/E_H$		$E_{2,s}/E_H$	
		odd	even	odd	even
0	29	.73	.25	.22	.16
1	22	.62	.14	.20	.14
2	19	.53	.08	.19	.13
3	16	.46	.00	.18	.12

Table 2 : Hydrogen binding energies (in units of  $E_H = -13.6$  ev) computed in variational calculation #1 for  $H = 10^{12}$  gauss.

s	$A_s$	$E_s/E_H$
0	1.99	11.9
1	1.66	9.40
2	1.48	8.11
3	1.36	7.29
4	1.27	6.69
5	1.20	6.24

REFERENCES

- Canuto, V., and Chiu, H. Y. 1968, Phys. Rev., 173, 1210.
- , and Kelly, D. C. (submitted to Nuovo Cimento).
- Chiu, H. Y., and Canuto, V. 1969, Phys. Rev. Ltrs., 22, 415.
- Cohen, R., Lodenquai, J., and Ruderman, M. 1970, Phys. Rev. Ltrs., 25, 467.
- Cox, J. P., and Giuli, R. T. 1968, Principles of Stellar Structure (New York: Gordon & Breach).
- Crawford, F. H. 1963, Heat, Thermodynamics, and Statistical Physics (New York: Harcourt, Brace & World, Inc.).
- Gradshteyn, I. S., and Ryzhik, I. M. 1965, Table of Integrals, Series, and Products (New York: Academic Press).
- Haines, L. K., and Roberts, D. H. 1969, Amer. J. Phys., 37, 1145.
- Kadomstev, B. B. 1970, JETP, 31, 945.
- Leighton, R. 1959, Principles of Modern Physics (New York: McGraw-Hill).
- Mathews, J., and Walker, R. L. 1965, Mathematical Methods of Physics (New York: W. A. Benjamin Inc.).
- Motz, L. 1970, Astrophysics and Stellar Structure (Waltham, Mass.: Ginn & Co.).

Part III

CYCLOTRON RADIATION IN AN  
INTENSE MAGNETIC FIELD

## Chapter 10

### INTRODUCTION

Parts I and II of this thesis dealt with the environment of a neutron star, particular attention being paid to the theoretically possible magnetic field of  $\sim 10^{12}$  gauss. In part III a different kind of star is considered, namely a white dwarf.

In 1970 circular polarization was discovered in the optical continuum radiation from the white dwarf Grw+70°8247 (Kemp et al. 1970). Subsequently a degree of circular polarization has been observed in the optical radiation from three other white dwarfs and some twenty other stars as well (Landstreet and Angel 1971).

The degree of circular polarization of G195-19 exhibits a sinusoidal variation with time, oscillating between 0 and .5 per cent with a period of about 32 hours in the blue-green (Angel and Landstreet 1971). The period is the same for other wave-lengths but the phase is not. Moreover the mean level shifts from the  $\sim .25\%$  in the blue-green to  $\sim .5\%$  in the UV and  $\sim .75\%$  in the red.

The higher percentages in the UV and red regions also appear in the spectrum of G99-37 (Landstreet and Angel 1971). Grw+70°8247 however, does quite the opposite as its degree of circular polarization drops off in the UV and red regions, having reached a peak at  $\sim 4500$  Å (Kemp 1970).

If one believes that the circular polarization arises from some

differential cyclotron mechanism, one concludes that there must be regions where the cyclotron frequency is in the optical range.

i.e. 
$$\omega_c = \frac{e\hbar}{mc} \sim 4 \times 10^{15} \quad (\approx 5000 \text{ \AA})$$

implying 
$$\hbar \approx 2.4 \times 10^8 \text{ gauss}$$

A magnetic field of  $\sim 10^8$  gauss is consistent with the consideration whereby a field of  $\sim 10^{12}$  gauss is suggested for a neutron star. Starting with  $\sim 100$  gauss and a radius of  $\sim 10^{11}$  cm., conservation of magnetic flux leads to  $\sim 10^8$  gauss for a radius of  $\sim 10^8$  cm. (typical white dwarf), and  $\sim 10^{12}$  gauss for a radius of  $\sim 10^6$  cm. (typical neutron star).

Some speculative attempts have been made to explain the various features of the circular polarization data. Kemp (1970) has suggested that the emission mechanism is an intermediate one somewhere between gray-body magnetoemission and super-quantized hydrogen emission (i.e. hydrogen with a Landau-like level structure as discussed in part II). The periodic variation with time is probably a manifestation of the star's rotation, with the magnetic axis of the active region at an angle to the axis of rotation of the star. The different phases for different wave-lengths perhaps indicate more than one active region. It is just such white dwarf "spots" that will be considered here.

In the following sections the circular polarization characteristics of some simple models are calculated:

- (1) a "thin" hemisphere with a radial magnetic field, viewed along its axis, assuming no absorption;
- (2) a "thin" hemisphere with a dipole-like magnetic field, viewed along its axis, assuming no absorption;
- (3) a "thin" flat sheet on a star's surface, viewed at various angles, assuming that the polarized component is  $\sim 1\%$  of the total flux at the particular wave-length being considered;
- (4) a layered atmosphere, viewed normal to the surface, assuming collisional absorption, and simple variation of temperature and magnetic field.

## Chapter 11

### THIN SHELL CYCLOTRON RADIATION

#### 11.1 General Formulation

For a completely polarized monochromatic wave propagating in the positive  $z$ -direction, the Stokes parameters are (Bekefi 1966)

$$\begin{aligned} F &= E_{ox}^2 + E_{oy}^2 \\ Q &= E_{oy}^2 - E_{ox}^2 \\ U &= 2 E_{ox} E_{oy} \cos \delta \\ V &= 2 E_{ox} E_{oy} \sin \delta \end{aligned} \tag{11.1}$$

where the wave's  $\vec{E}$  vector is defined by

$$\begin{aligned} E_x(t) &= E_{ox} e^{i(\omega t - \phi_1)} \\ E_y(t) &= E_{oy} e^{i(\omega t - \phi_2)} \\ \delta &= \phi_1 - \phi_2 \end{aligned} \tag{11.2}$$

The degree of polarization  $p$  is then given by



$$P = \frac{\sqrt{Q^2 + U^2 + V^2}}{F} \quad (11.3)$$

For circularly polarized waves,  $E_x(t)$  and  $E_y(t)$  must be equal in magnitude and  $90^\circ$  out of phase.

i.e.  $E_{ox} = E_{oy} \quad (11.4)$

and  $\delta = \pm \pi/2 \quad (11.5)$

Then  $Q = U = 0 \quad (11.6)$

and  $P^{CP} = \frac{V}{F} \equiv \left| \frac{F^R - F^L}{F^R + F^L} \right| \quad (11.7)$

where  $P^{CP}$  is the degree of circular polarization and  $F^R$  and  $F^L$  are the fluxes of the right-hand and left-hand circularly polarized waves respectively.

If two incoherent beams are added, their Stokes parameters are additive. Therefore the radiation emitted in a direction  $\vec{l}$  by a thin shell with surface  $S$  will have a net degree of circular polarization given by

$$\langle P^{CP} \rangle = \frac{\int_S V da_1}{\int_S F da_1} \quad (11.8)$$

where 
$$da_{\perp} = \vec{n} \cdot \vec{\ell} \, r^2 \sin \theta \, d\theta \, d\phi \quad (11.9)$$

in spherical polar coordinates, and  $\vec{n}$  is the unit normal outward to the surface.

The coefficient  $\eta_{\omega}$  of spontaneous emission for the cyclotron emission of an electron is (Bekefi 1966)

$$\eta_{\omega}(\omega, \nu, \theta) = \frac{e^2 \omega^2}{2\pi c} \sum_{m=1}^{\infty} \left| \begin{array}{c} -\hat{x} \frac{\cos \theta}{\sin \theta} (\cos \theta - \beta_{\parallel}) J_m(x) \\ -\hat{y} i\beta_{\perp} \frac{dJ_m(x)}{dx} \\ \hat{z} (\cos \theta - \beta_{\parallel}) J_m(x) \end{array} \right|^2 S(y) \quad (11.10)$$

where

$$\begin{aligned} x &= \frac{\omega}{\omega_c} \beta_{\perp} \sin \theta \\ y &= m\omega_c - \omega(1 - \beta_{\parallel} \cos \theta) \\ \omega_c &= \frac{eB}{m_0 c} \sqrt{1 - \beta^2} \\ \beta &= v/c = \left[ \left( \frac{v_{\parallel}}{c} \right)^2 + \left( \frac{v_{\perp}}{c} \right)^2 \right]^{1/2} \end{aligned} \quad (11.11)$$

with the magnetic field  $\vec{B}$  along the positive z-direction and the photon propagation vector  $\vec{k}$  in the x-z plane (see Figure 1).

$\eta_{\omega}(\omega, \nu, \theta)$  is the differential rate at which energy is emitted in

the direction  $\theta$  as defined in Figure 1, per unit solid angle, per unit frequency interval  $d\omega$ , by an electron with a velocity in the interval  $(v, v+dv)$ . The emission coefficient  $j_\omega$  is obtained by integrating  $\eta_\omega$  over the velocity distribution  $f(v)$ .

i.e

$$j_\omega = \int \eta_\omega(\omega, v, \theta) f(v) d^3v \quad (11.12)$$

In the expression for  $\eta_\omega(\omega, v, \theta)$ , 'm' categorizes the particular cyclotron harmonics.

$$\omega = \frac{m\omega_c}{1 - \beta_{||} \cos \theta} \quad (11.13)$$

where

$$\omega_c = \frac{e\hbar}{m_0 c} \sqrt{1 - \beta^2}$$

For a particular 'm',  $\eta_\omega$  reduces to

$$\eta_m(v, \theta) = \frac{e^2 \omega_m^2}{2\pi c} \left( \frac{\cos \theta - \beta_{||}}{\sin \theta} \right)^2 \left[ J_m^2(x) + \beta_\perp^2 J_m'^2(x) \right] \quad (11.14)$$

In the non-relativistic region (i.e.  $m/\beta \ll 1$ ), the total radiation of a harmonic is

$$\eta_m^\pi = \frac{2e^2 \omega_c^2}{c} \frac{(m+1)m^{2m+1}}{(2m+1)!} \beta^{2m} \quad (11.15)$$

Then

$$\frac{\eta_m^\pi}{\eta_{m+1}^\pi} = \left( \frac{c}{v} \right)^2 \gg 1 \quad (11.16)$$

Thus, to order  $\beta^2$ , only the first harmonic need be considered.

The non-relativistic condition also means 'x' is small, thereby allowing the approximations

$$J_1(x) \approx \frac{1}{2} x \quad (11.17)$$

and

$$J_1'(x) \approx \frac{1}{2}$$

Therefore, the non-relativistic form of  $\eta_\omega$  is

$$\eta_\omega(\omega, \nu, \theta) \approx \frac{e^2 \omega}{4\pi c} \beta_\perp \begin{vmatrix} -\hat{x} \cos \theta (\cos \theta - \beta_\parallel) \\ -\hat{y} i \\ \hat{z} \sin \theta (\cos \theta - \beta_\parallel) \end{vmatrix}^2 \delta(\omega - \omega_c) \quad (11.18)$$

The vector in the above  $\eta_\omega$  expression has been retained because its direction and phase are those of the photon's electric vector  $\vec{E}$  (i.e the polarization information for the process). Thus the photon's electric vector  $\vec{E}$  is, aside from constants, given by

$$\vec{E} \sim \beta_\perp (-\cos \theta (\cos \theta - \beta_\parallel), -i, \sin \theta (\cos \theta - \beta_\parallel)) \quad (11.19)$$

In order to obtain the Stokes parameters of this wave,  $\vec{E}$  must be resolved along directions perpendicular to the propagation vector  $\vec{k}$ . The easiest choices are  $\hat{e}_y$  and  $\hat{e}_y \times \vec{k}$  defining  $E_1^{(2)}$  and  $E_1^{(1)}$  respectively. i.e.

$$E_1^{(1)} \sim -(\cos \theta - \beta_\parallel) \beta_\perp$$

$$E_1^{(2)} \sim -i\beta_1 \quad (11.20)$$

Therefore, for equations (11.1) we have

$$"E_{ox}" \sim (\cos \theta - \beta_{||}) \beta_1 \quad (11.21)$$

$$"E_{oy}" \sim \beta_1$$

$$"s" \sim \pi/2$$

i.e.

$$\begin{aligned} F &\propto [1 + (\cos \theta - \beta_{||})^2] \beta_1^2 \\ V &\propto 2(\cos \theta - \beta_{||}) \beta_1^2 \end{aligned} \quad (11.22)$$

The degree of circular polarization of the cyclotron emission of an ensemble of electrons is then

$$\langle P^{CP} \rangle = \frac{2 \langle (\cos \theta - \beta_{||}) \beta_1^2 \rangle}{\langle [1 + (\cos \theta - \beta_{||})^2] \beta_1^2 \rangle} \quad (11.23)$$

where the brackets indicate a summation over the ensemble.

The type of ensemble that will be considered in detail is a thin shell of electrons in which  $\beta_1$  is constant throughout and  $\langle \beta_{||} \rangle = 0$  (i.e. no net drift).  $\langle \beta_{||}^2 \rangle$  can also be neglected since it is much less than 1 for the non-relativistic case. Then

$$\langle P^{CP} \rangle_{\text{shell}} \propto \frac{2 \langle \cos \theta \rangle}{1 + \cos^2 \theta} \quad (11.24)$$

where

$$\cos \Theta = \frac{\vec{r}_b \cdot \vec{l}}{|\vec{r}_b|} \quad (11.25)$$

For such an emitting surface

$$\langle p^{cr} \rangle_{\text{shell}} \approx \frac{2 \int_S \frac{\vec{r}_b \cdot \vec{l}}{|\vec{r}_b|} \vec{n} \cdot \vec{l} \, da}{\int_S \left[ 1 + \left( \frac{\vec{r}_b \cdot \vec{l}}{|\vec{r}_b|} \right)^2 \right] \vec{n} \cdot \vec{l} \, da} \quad (11.26)$$

## 11.2 Hemispherical Shell and a Radial Magnetic Field

A simple example of a magnetic shell is a hemisphere with a radially symmetric magnetic field (see Figure 2). Then

$$\begin{aligned}\vec{n} &= \frac{\vec{H}}{|\vec{H}|} = (\sin \theta \cos \phi, \sin \theta \sin \phi, \cos \theta) \\ \vec{\ell} &= (0, 0, 1) \\ da &= r^2 \sin \theta \, d\theta \, d\phi\end{aligned}\tag{11.27}$$

Using equation (11.26) gives

$$\langle P^{cp} \rangle = \frac{2 \int_0^{\pi/2} d\theta \int_0^{2\pi} d\phi \cos^2 \theta \sin \theta}{\int_0^{\pi/2} d\theta \int_0^{2\pi} d\phi (1 + \cos^2 \theta) \sin \theta \cos \theta}\tag{11.28}$$

i.e.  $\langle P^{cp} \rangle \approx 90\%$

Thus the cyclotron radiation emitted by such a thin shell of electrons has a degree of circular polarization of about 90%.

### 11.3 Hemispherical Shell and a Dipole-like Magnetic Field

Suppose a dipole magnetic field is mapped onto a hemisphere as shown in Figure 3. Then

$$\frac{\vec{H}}{|\vec{H}|} = \frac{1}{(3\cos^2\theta + 1)^{1/2}} (3\sin\theta\cos\theta\cos\phi, 3\sin\theta\cos\theta\sin\phi, 3\cos^2\theta - 1) \quad (11.29)$$

with the dipole axis along the positive z-axis. Without loss of generality the line of sight  $\hat{l}$  can be put in the x-z plane at an angle  $\Theta$  to the z-axis.

i.e.

$$\hat{l} = (\sin\Theta, 0, \cos\Theta) \quad (11.30)$$

The  $\Theta = 0$  case is straightforward as in section 11.2 .

$$\langle P^{CP} \rangle_{\Theta=0} \approx \frac{2 \int_0^{\pi/2} d\theta \int_0^{2\pi} d\phi \frac{(3\cos^2\theta - 1)}{(3\cos^2\theta + 1)^{1/2}} \sin\theta \cos\theta}{\int_0^{\pi/2} d\theta \int_0^{2\pi} d\phi \left[ 1 + \frac{(3\cos^2\theta - 1)^2}{3\cos^2\theta + 1} \right] \sin\theta \cos\theta} \quad (11.31)$$

Let

$$u = 3\cos^2\theta + 1 \quad (11.32)$$

Then

$$\langle P^{CP} \rangle_{\Theta=0} \approx \frac{2 \int_1^4 \frac{u-2}{\sqrt{u}} du}{\int_1^4 \left[ 1 + \frac{(u-2)^2}{u} \right] du}$$



$$\approx 1/3$$

(11.33)

Thus the cyclotron radiation emitted parallel to the dipole axis by a hemispherical shell with a dipole-like magnetic field configuration has a 33% degree of circular polarization. For  $\Theta \neq 0$ ,  $\langle P^{\text{cr}} \rangle$  will be different of course, as would be the case for off-axis viewing of the shell in the previous section. The computation is complicated by some of the radiation having to traverse the shell. It is simpler to just deal with a thin planar disk.

#### 11.4 A "Thin" Sheet

If we look at a flat layer of electrons emitting cyclotron radiation as pictured in Figure 4, the degree of circular polarization is simply

$$\langle P^{CP} \rangle = \frac{2 \cos \Theta}{1 + \cos^2 \Theta} \quad (11.34)$$

Suppose this small active region is on the surface of a star with coordinates as defined in Figure 4. Then

$$\cos \Theta = \sin \alpha \sin \xi \cos(\omega t + \phi_0) + \cos \alpha \cos \xi \quad (11.35)$$

since

$$\begin{aligned} \frac{\vec{H}}{|\vec{H}|} &= (\sin \alpha \cos \Phi, \sin \alpha \sin \Phi, \cos \alpha) \\ \vec{l} &= (\sin \xi, 0, \cos \xi) \end{aligned} \quad (11.36)$$

$$\Phi(t) = \omega t + \phi_0$$

and

$$\cos \Theta = \frac{\vec{H} \cdot \vec{l}}{|\vec{H}|}$$

Then

$$\langle P^{CP} \rangle = \frac{2A \cos(\omega t + \phi_0) + 2B}{1 + [A \cos(\omega t + \phi_0) + B]^2} \quad (11.37)$$

where

$$\begin{aligned} A &= \sin \alpha \sin \xi \\ B &= \cos \alpha \cos \xi \end{aligned} \quad (11.38)$$

Thus, as the star rotates, the degree of circular polarization varies. If  $A$  is small, the variation with time is essentially sinusoidal.

i.e.

$$\langle P^{cp} \rangle = \left( \frac{2A}{1+B^2} \right) \cos(\omega t + \phi_0) + \left( \frac{2B}{1+B^2} \right) \quad (11.39)$$

This degree of circular polarization is diluted by the unpolarized background radiation at the same frequency. Let the polarized flux be  $\eta$  % of the total flux at the cyclotron frequency. This percentage reflects the relative area of the active region and the various processes contributing flux. So

$$\langle P^{cp} \rangle = \left( \frac{2\eta A}{1+B^2} \right) \cos(\omega t + \phi_0) + \left( \frac{2\eta B}{1+B^2} \right) \quad (11.40)$$

It is interesting to take a semi-quantitative look at this model using actual white dwarf data. The data of G195-19 in the UV indicate (Angel and Landstreet 1971)

$$\frac{2\eta A}{1+B^2} \approx .25 \%$$

$$\frac{2\eta B_1}{1+B^2} \approx .5\% \quad (11.41)$$

An estimate is now needed for  $\eta$ . If the "spot" covers 10% of the star's disk, and if the cyclotron mechanism is a 10% component of the flux, then  $\eta \sim 1\%$ . Applying this guess to equations (11.41) gives

$$\begin{aligned} \frac{2A}{1+B^2} &\approx .25 \\ \frac{2B}{1+B^2} &\approx .5 \end{aligned} \quad (11.42)$$

The latter equation is easily solved.

i.e.

$$B \approx .27 \quad (11.43)$$

Then

$$A \approx .135 \ll 1$$

Therefore

$$\begin{aligned} \sin \alpha \sin \xi &\approx .135 \\ \cos \alpha \cos \xi &\approx .27 \end{aligned} \quad (11.44)$$

i.e.

$$\begin{aligned} \alpha &\approx 74^\circ \\ \xi &\approx 8^\circ \end{aligned} \quad (11.45)$$

Thus an active region, whose cyclotron radiation is  $\sim 1\%$  of the total flux at that frequency, oriented at an angle of  $74^\circ$ , and

viewed at an angle of  $8^\circ$ , (angles relative to the star's axis of rotation), can account for the degree of circular polarization of G195-19 in the UV.

Of course this approach is hopelessly simplistic, as it ignores temperature and magnetic field gradients, absorption, thermal equilibrium, a thick atmosphere, etc. etc. These factors will get some attention in the next section. Nevertheless, the above approach does provide some insight into the problem, particularly the sinusoidal variation and the percentage factor  $\eta$  .

## 11.5 An "Atmosphere"

It is evident from the simple calculations made in previous sections that an electron shell of constant  $|\vec{H}|$  can produce a significant degree of circular polarization in its cyclotron emission. Unfortunately, if the shell is isothermal and in thermal equilibrium, no net polarization can arise. However, if there are temperature and magnetic field gradients such that the emission and absorption take place at different temperatures, a net polarization can occur.

This possibility can be investigated by considering a section of atmosphere, the usual plasma relations for cyclotron emission and absorption, and radiative transfer under equilibrium conditions.

The absorption coefficient of left-handed circularly polarized waves (i.e. ordinary waves) is given by the relation (Bekefi 1966)

$$\alpha_{\omega}^L \approx \frac{1}{c} \left[ \frac{\omega_p^2 \nu}{(\omega + \omega_c)^2 + \nu^2} \right] \quad (11.46)$$

where  $\omega_p$  is the plasma frequency,  $\omega_c$  is the cyclotron frequency, and  $\nu$  is the collision frequency.

i.e

$$\omega_p^2 = \frac{4\pi N_e e^2}{m} \quad (11.47)$$

and

$$\omega_c = \frac{e H_0}{mc}$$

As an estimate of the relative magnitude of these frequencies we can substitute "typical" conditions like (Motz 1970)

$$\begin{aligned} N_e &\approx 10^{15} \text{ cm}^{-3} \\ T &\approx 10^4 \text{ }^\circ\text{K} \\ \omega &\approx 10^{15} \text{ sec}^{-1} \approx \omega_c \end{aligned} \quad (11.48)$$

Then 
$$\omega_p^2 \approx 3 \times 10^{24} \quad (11.49)$$

and 
$$\omega_p^2 \ll \omega^2$$

The collision frequency can be estimated from the usual bremsstrahlung result (Bekefi 1966)

$$\nu_{\text{eff}} = 6.6 \frac{Z N_e \bar{G}}{T^{3/2}} \quad (11.50)$$

where  $\bar{G}$  is the Gaunt factor given by

$$\bar{G}(T, \omega) = \frac{\sqrt{3}}{\pi} \left[ 19.56 + \ln \frac{T^{3/2}}{\omega Z} \right] \quad (11.51)$$

The result for the above conditions and  $Z=1$  is

$$\nu \approx 10^{11} \text{ sec}^{-1} \quad (11.52)$$

i.e.

$$\nu \ll \omega_p \ll \omega \sim \omega_c \quad (11.53)$$



and 
$$\alpha_{\omega_c}^L \approx \frac{\omega_p^2 \nu}{4c\omega_c^2} \approx 2.5 \times 10^{-6} \text{ cm}^{-1} \quad (11.54)$$

Thus the ordinary wave absorption is very low.

In contrast, the extraordinary wave undergoes resonance absorption.

Its absorption coefficient is

$$\alpha_{\omega}^R = \frac{1}{c} \left[ \frac{\omega_p^2 \nu}{(\omega - \omega_c)^2 + \nu^2} \right] \quad (11.55)$$

For  $\omega_p^2 \approx 3 \times 10^{24}$ ,  $\nu \approx 10^{11}$

$$\alpha_{\omega_c}^R \approx \frac{\omega_p^2}{c\nu} \approx 10^3 \text{ cm}^{-1} \quad (11.56)$$

Thus in the region where  $\omega \sim \omega_c$  the extraordinary wave is absorbed very strongly (see Figure 5). Such a layer then acts as a polarizer.

As a simple model to illustrate this polarizing mechanism, consider a layer of electrons with parameters  $\omega_c, T, N_e$  varying in the manner shown in Figure 6. Furthermore, let us assume Maxwellian velocity distributions and no incident radiation on the layer.

The radiation that emerges normal to the layer's surface is given by the solution to the equation of radiative transfer. For normal propagation and no incident radiation this solution is simply

$$I_{\omega} = \int_0^{\tau_0} S_{\omega}(\tau) e^{-\tau} d\tau \quad (11.57)$$



where

$$\tau = \int_0^z \alpha_\omega dz$$

$$\tau_0 = \int_0^L \alpha_\omega dz$$
(11.58)

and  $S_\omega$  and  $\alpha_\omega$  are the source function and absorption coefficient respectively. For the case of a Maxwellian velocity distribution the source function  $S_\omega$  is the Planck function  $B_\omega(T)$ .  
i.e.

$$S_\omega(\tau) = \frac{\hbar\omega^3}{8\pi^3c^2} \frac{1}{e^{\frac{\hbar\omega}{kT}} - 1} \approx \frac{\omega^2}{8\pi^3c^2} kT$$
(11.59)

[ $\hbar\omega \ll kT$ ]

which is the usual Rayleigh-Jeans approximation.

Therefore

$$I_\omega \approx \frac{\omega^2 k}{8\pi^3 c^2} \int_0^{\tau_0} T(\tau) e^{-\tau} d\tau$$
(11.60)

This integral must be evaluated for both polarizations, with

$$\tau^L = \int_0^z \alpha_\omega^L dz$$

$$\tau^R = \int_0^z \alpha_\omega^R dz$$
(11.61)

A reasonable approximation is to treat  $\alpha_\omega^L$  as essentially constant

and small over the entire region. Then

$$\tau_{\omega}^L \approx \alpha_{\omega}^L z \quad (11.62)$$

and

$$\tau_0^L \approx \alpha_{\omega}^L L \quad (11.63)$$

For this model

$$T(z) = T_0 \exp\left(\frac{z}{L} - 1\right) \quad (11.64)$$

Therefore

$$\begin{aligned} I_{\omega}^L &\approx \frac{\omega^2 k}{8\pi^3 c^2} \int_0^L T_0 \exp\left(\frac{z}{L} - 1\right) e^{-\alpha_{\omega}^L z} \alpha_{\omega}^L dz \\ &\approx \frac{\omega^2 k}{8\pi^3 c^2} \frac{T_0 \alpha_{\omega}^L}{e} \int_0^L \exp\left[\left(\frac{z}{L} - \alpha_{\omega}^L\right)z\right] dz \\ &= \frac{\omega^2 k}{8\pi^3 c^2} \frac{T_0 \alpha_{\omega}^L L}{e} \frac{[\exp(z - \alpha_{\omega}^L L) - 1]}{(z - \alpha_{\omega}^L L)} \quad (11.65) \end{aligned}$$

For  $\int_{\omega}^R$  the resonance region  $\omega \sim \omega_c$  is virtually an infinite absorber. Moreover, outside this region

$$\alpha_{\omega}^R \approx \alpha_{\omega}^L \quad (11.66)$$

Therefore

$$I_{\omega}^R \approx \frac{\omega^2 k}{8\pi^3 c^2} \frac{T_0 \alpha_{\omega}^L L}{e} \frac{\exp\left(2\frac{L^*}{L} - \alpha_{\omega}^L L^*\right) - 1}{(2 - \alpha_{\omega}^L L)} \quad (11.67)$$

where  $L^*$  is defined by

$$\omega = \omega_0 \exp\left(2\frac{L^*}{L} - 1\right) \quad (11.68)$$

and

$$L^* = \frac{1}{2} \left[ 1 + \ln\left(\frac{\omega}{\omega_0}\right) \right] L \quad (11.69)$$

Finally

$$\langle P^{cp} \rangle_{\omega} = \frac{\exp(2 - \alpha_{\omega}^L L) - \exp\left(2\frac{L^*}{L} - \alpha_{\omega}^L L^*\right)}{\exp(2 - \alpha_{\omega}^L L) + \exp\left(2\frac{L^*}{L} - \alpha_{\omega}^L L^*\right) - 2} \quad (11.70)$$

Figure 7 shows the variation of  $\langle P^{cp} \rangle_{\omega}$  with frequency  $\omega$  for

$$\alpha_{\omega}^L \approx 2.5 \times 10^{-6} \text{ cm}^{-1}$$

and

$$L \approx 10^6 \text{ cm} \quad (11.71)$$

since white dwarf atmospheres generally have a depth from 1% to 10% of the star's radius (Motz 1970).

The decrease of  $P$  with increasing  $\omega$  is similar to the behaviour derived by Kemp (1970) in his gray-body magnetoemission theory (i.e.

$p \propto \lambda$  ). The outer "edge" of the atmosphere could supposedly provide a low frequency cutoff for the polarizing mechanism as both absorption coefficients drop to zero. Finally, the degree of circular polarization from the whole star brings back the need for the factor  $\eta$  representing the ratio of the spot's flux to that of the whole disk.

## Chapter 12

### CONCLUSIONS AND DISCUSSION

Simple models of cyclotron active regions on the surface of white dwarfs can account for some of the qualitative and quantitative aspects observed in the degree of circular polarization of their optical emission. A spot with a magnetic field oblique to the star's rotational axis can give a sinusoidal dependence. A spot with a temperature and magnetic field gradient can give a wave-length dependence. A series of spots can account for the phase differences at different wave-lengths.

Some sort of combination of the models presented in sections 11.2 through 11.5 might be the answer, though the complexities of oblique propagation, non-layering, etc. would make a thorough investigation very arduous. An obvious improvement would be the use of a theoretical white dwarf atmosphere model.

Other mechanisms are of course possible. Kemp (1970) suggests a magnetic breakdown in hydrogen resulting in a series of Landau-like levels as has been suggested for hydrogen in  $\sim 10^{12}$  gauss.  $10^8$  gauss is a rather difficult intermediate case unfortunately. Moreover, there still remains the problem of different time phases of these supposed Landau harmonics.

There is also the question of linear polarization. It has been

observed in the white dwarf optical emission and is an order of magnitude smaller (Kemp 1970). Linear polarization usually suggests a transverse  $\vec{E}$  component. Sections 11.2 to 11.4 could be extended to look at linear polarization effects.

As a final note, circular polarization has been observed in Jupiter's decimetric emission (Komesaroff et al. 1970). "Thin" shell synchrotron radiation has been favoured as the source mechanism, thereby predicting a surface polar field strength of between 22 and 100 gauss.

Thus these polarization and magnetic effects cover a lot of territory :- ten orders of magnitude in magnetic field strength, radiation via bremsstrahlung, hydrogen transitions, cyclotron and synchrotron mechanisms, and astronomical entities such as neutron stars, white dwarfs, and planets. This thesis has described some of my efforts in this vast subject area.



Figure 2: Hemispherical Shell and a Radial Magnetic Field

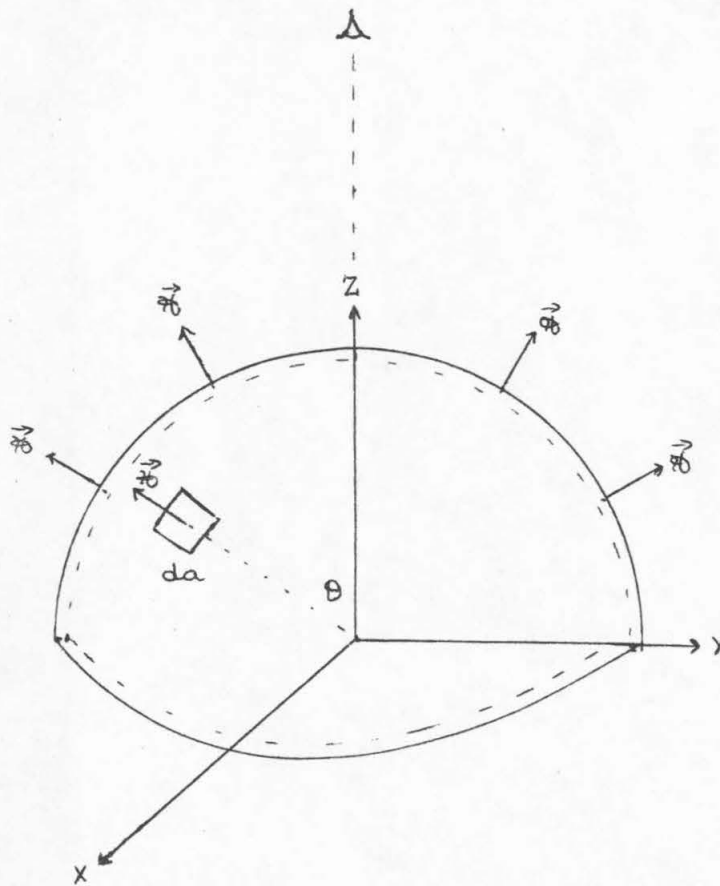




Figure 3: Hemispherical Shell and a Dipole-like Magnetic Field

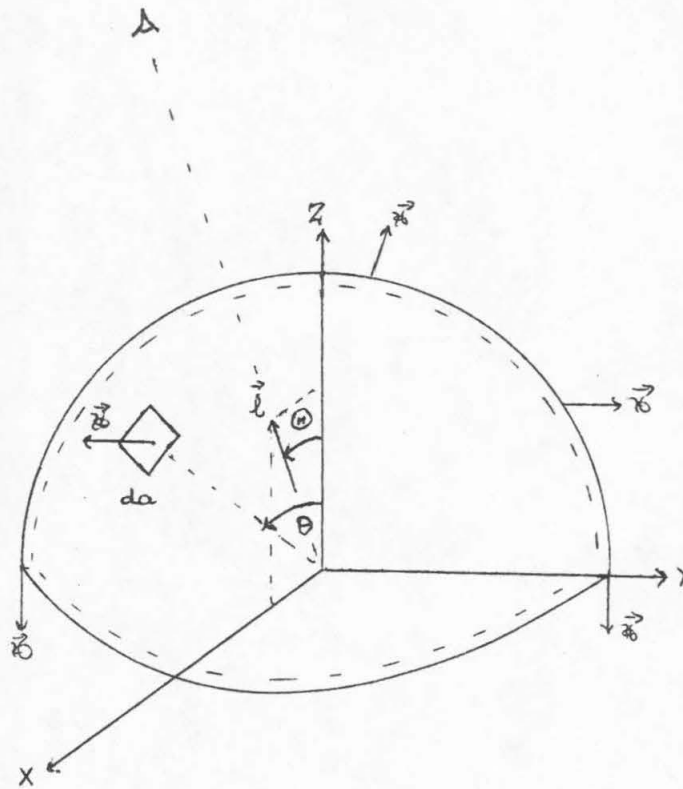


Figure 4: A Thin Spot on a Star's Surface

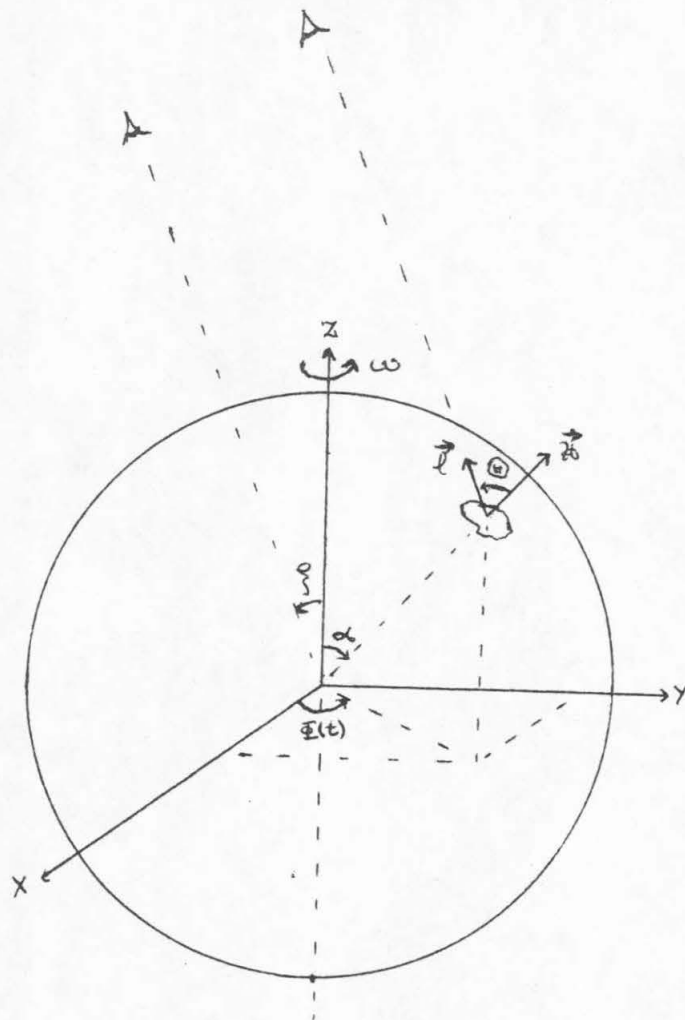


Figure 5: Cyclotron Absorption Coefficients

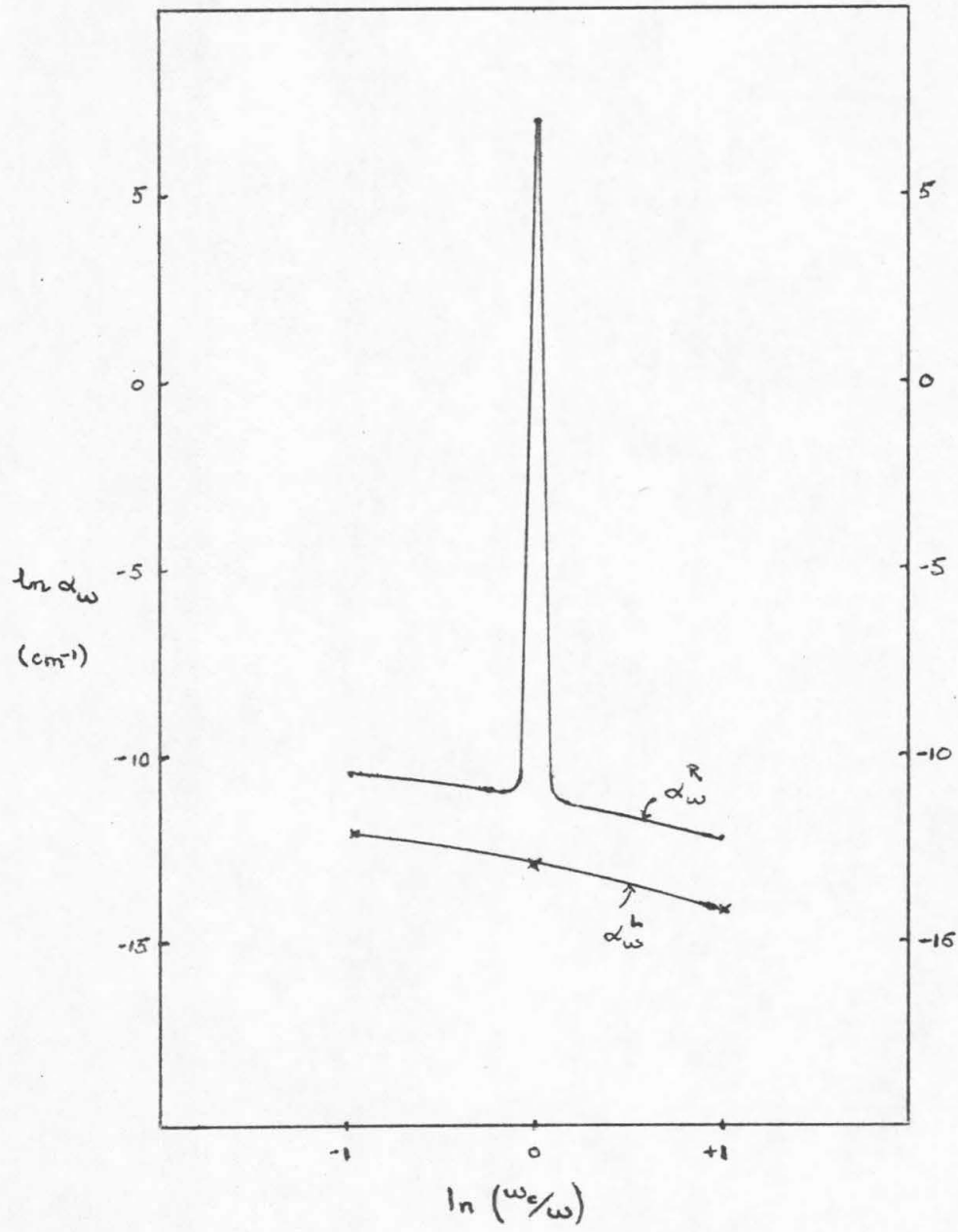


Figure 6: An Atmospheric Layer

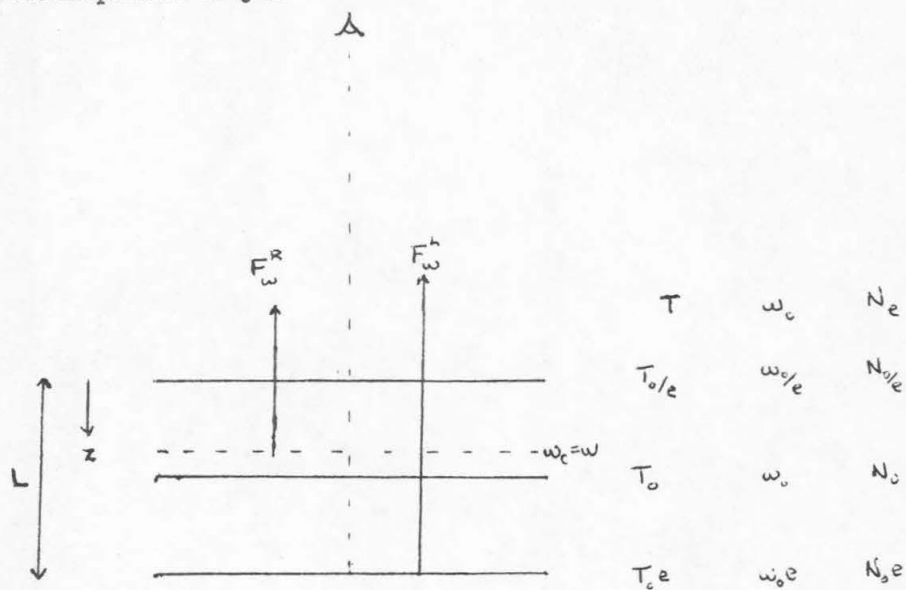
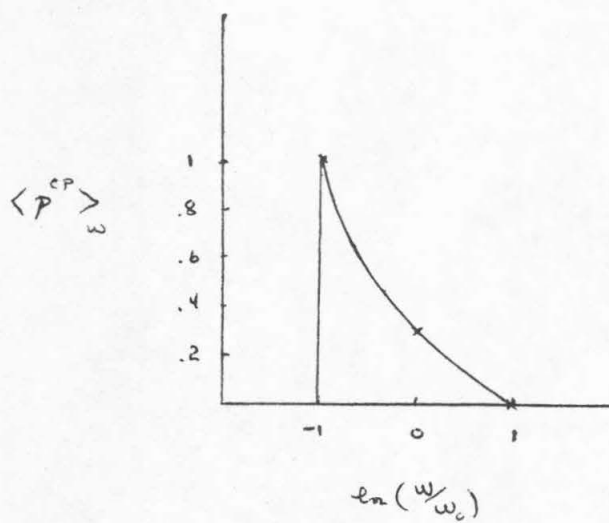


Figure 7: Circular Polarization vs. Frequency



REFERENCES

- Angel, J. R. P., and Landstreet, J. D. 1971, Ap. J. (Letters), 165, L71.
- Bekefi, G. 1966, Radiation Processes in Plasmas (New York: John Wiley & Sons, Inc.).
- Kemp, J. C. 1970, Ap. J. (Letters), 162, L69.
- Kemp, J. C., Swedlund, J. B., Landstreet, J. D., and Angel, J. R. P. 1970, Ap. J. (Letters), 161, L77.
- Komesaroff, M. M., Morris, D., and Roberts, J. A. 1970, Astrophys. Ltrs., 7, 31.
- Landstreet, J. D., and Angel, J. R. P. 1971, Ap. J. (Letters), 165, L67.
- Motz, L. 1970, Astrophysics and Stellar Structure (Waltham, Mass.: Ginn & Co.).